Preserving the validity of the two-Higgs-doublet model up to the Planck scale

P. M. Ferreira[*]

ISEL - Instituto Superior de Engenharia de Lisboa, Instituto Politécnico de Lisboa, Portugal
and Centro de Física Teórica e Computacional, Faculdade de Ciências, Universidade de Lisboa, Portugal

Howard E. Haber[†] and Edward Santos[‡]

Santa Cruz Institute for Particle Physics, University of California, Santa Cruz, California 95064, USA

We examine the constraints on the two-Higgs-doublet model (2HDM) due to the stability of the scalar potential and absence of Landau poles at energy scales below the Planck scale. We employ the most general 2HDM that incorporates an approximately Standard Model (SM) Higgs boson with a flavor aligned Yukawa sector to eliminate potential tree-level Higgs-mediated flavor changing neutral currents. Using basis independent techniques, we exhibit regimes of the 2HDM parameter space with a 125 GeV SM-like Higgs boson that is stable and perturbative up to the Planck scale. Implications for the heavy scalar spectrum are exhibited.

I. INTRODUCTION

With the recent discovery of a Higgs-like particle with a mass of about 125 GeV by both the ATLAS [1] and CMS [2] collaborations, the focus has now turned to deciphering the properties of this particle and determining whether it is the Standard Model (SM) Higgs particle, or part of an extended Higgs sector. Analyses performed by ATLAS and CMS collaborations have shown that the couplings of the newly discovered particle are consistent with a SM-like Higgs boson, within the accuracy of their measurements. In light of the present precision of the Higgs data, the LHC can claim to have discovered a SM-like Higgs boson. However, there is still plenty of room for deviations from SM behavior of $\mathcal{O}(10\%)$. A SM-like Higgs boson is easily achieved in an extended Higgs sector in the decoupling limit, where the lightest scalar is identified as the observed SM-like Higgs boson, and the heavier scalars are somewhat separated in mass (e.g. with a mass scale above 350 GeV [3,4]).

Before the mass of the Higgs boson was known, upper bounds on the SM Higgs mass were obtained by requiring that the running quartic coupling parameter avoid Landau poles (LPs); i.e., the coupling was required to remain finite up to a given energy scale Λ [5–7]. Lower bounds were obtained by requiring that the scalar potential remain stable during renormalization group (RG) evolution [8–13]. That is, the scalar potential is bounded from below at all scales between the electroweak scale and Λ. These bounds were contingent on the assumption that no new physics beyond the SM (BSM) enters between the electroweak scale and Λ. Turning around the argument, the existence of a LP or an instability of the scalar potential at some energy scale Λ suggests that new BSM physics must be present at or below Λ.

After the discovery of the Higgs boson, previously obtained bounds were updated using two-loop renormalization group equations (RGEs) in Ref. [14] and three-loop RGEs by Ref. [15]. The most recent analysis of Ref. [16] has shown that the SM scalar potential becomes unstable at a value of Λ well below the Planck scale, if the Higgs boson mass is smaller than 129.6 ± 1.5 GeV.[1] Taken at face value, these results would further imply that we live in a metastable vacuum that will eventually (and catastrophically) decay via tunneling into the true vacuum. However, the lifetime of the metastable vacuum is many orders of magnitude larger than the age of the universe [16,17]. On the other hand, if the electroweak vacuum is absolutely stable, then the recent LHC discovery of a 125 GeV SM-like Higgs boson requires the existence of new BSM physics at an energy scale below a scale of $\Lambda \simeq 10^{9.5}$ GeV, where there is an uncertainty of about 1 in the exponent due to parametric uncertainties of m_t, α_s and the Higgs mass [16], in order to avoid the metastability of the SM vacuum.

Although the prospect of existence of new BSM physics is exciting, there is no guarantee that the scale of the new physics is close to the electroweak scale. Nevertheless, arguments motivated by naturalness of the electroweak symmetry breaking (EWSB) mechanism suggest that BSM physics should be present at or near the TeV scale (see e.g., Refs. [18,19] for a review and a guide to the literature). Many models of new physics have been proposed to address the origin of ESWB, and many of these approaches

---

[*]ferreira@cii.fc.ul.pt
[†]haber@scipp.ucsc.edu
[‡]edrsanto@ucsc.edu

[1]The quoted uncertainty takes into account the parametric uncertainty of m_t and α_s and the effects of unknown higher order corrections [16].

possess extended Higgs sectors. However, in such models one must specify the BSM physics in order to study the behavior of running couplings between the electroweak scale and some very high energy scale Λ. At present, there is no direct experimental evidence that the origin of the EWSB scale is a consequence of naturalness. Adding additional Higgs multiplets at or near the TeV scale by themselves does not address the origin of EWSB. Indeed, one could argue that it makes matters worse by adding additional fine-tuning constraints. Nevertheless, in this paper we shall accept the fine-tunings required to sustain an extended Higgs sector near the TeV scale. After all, we know that multiple generations exists in the fermionic sector of the Standard Model. Thus, we should be prepared for the possibility that the scalar sector of the theory is also nonminimal.

Here, we shall focus on the two-Higgs-doublet model (2HDM), which was initially proposed by Lee in 1973 [20] (for a review, see e.g. Ref. [21]). It provides a richer Higgs particle spectrum, namely three neutral scalars and a charged pair. The 2HDM admits the possibility of CP-violation in the scalar potential, both explicit or spontaneous. In the limit of CP-conservation, two of the neutral scalars are CP-even, typically denoted by h and H, (where $m_h < m_H$) while the other neutral scalar is CP-odd, denoted by A. We shall consider a very general version of the 2HDM that is not inconsistent with present data. Such a model must possess a SM-like Higgs boson (within the accuracy of the present Higgs data). In addition, Higgs-mediated tree-level flavor changing neutral currents (FCNCs) must be either absent or highly suppressed. These conditions are achieved if the nonminimal Higgs states of the model have masses above about 350 GeV and if the Yukawa couplings are aligned in such a way that the neutral Higgs couplings are diagonal in the mass-basis for the neutral Higgs bosons. The most general 2HDM parameter space allowed by the present data is somewhat larger than the one specified here. Nevertheless, the restricted parameter space outlined above is still quite general and incorporates the more constrained 2HDMs considered in the literature.

The existence of additional scalar degrees of freedom in an extended Higgs sector provides an opportunity to cure the vacuum metastability problem of the SM Higgs boson. However, by demanding no Landau poles and requiring a stable scalar potential at all energy scales up to the Planck scale, one imposes strong constraints on the parameter space of the extended Higgs sector. Investigations of this type have been performed in extended Higgs sectors prior to the discovery of the Higgs boson in Refs. [22–28]. With the discovery and identification of a SM-like Higgs boson, the question of the validity of extended Higgs sectors up to the Planck scale has become more focused. A number of authors have considered the stability properties of extended Higgs sectors with additional singlet scalar fields [29–32] and 2HDMs with constrained scalar potentials [33–35].

In this paper, we examine the theoretical consistency of *the most general* 2HDM between the electroweak scale and the Planck scale, using the one-loop RGEs of the model to investigate the possible occurrence of Landau poles and instability of the scalar potential. We focus on the decoupling regime of the 2HDM where the 125 GeV Higgs boson is SM-like [36,37], and assume Yukawa alignment in the flavor sector [38] to avoid Higgs-mediated tree-level FCNCs. Our aim is to exhibit the allowed regions of the 2HDM parameter space that are free from both Landau poles and vacuum instability below the Planck scale. In particular, a 2HDM that satisfies these constraints does not require further BSM physics to stabilize the theory.

One of the distinguishing features of the most general 2HDM is the fact that the two scalar doublet, hypercharge-one fields are indistinguishable. One is always free to define new linear combinations of the scalar doublets that preserve the kinetic energy terms of the Lagrangian. A specific choice for the scalar fields is called a *basis*, and any physical prediction of the theory must be *basis indepen-dent*. In our analysis, we employ a basis-independent formalism introduced in Ref. [39]. We consider the most general 2HDM scalar potential (which is potentially CP-violating) and the most general Yukawa sector, which introduces three additional independent 3×3 matrix Yukawa couplings. Without additional assumptions, the latter yields Higgs-mediated tree-level FCNCs, in conflict with observed data. In order to circumvent this, we impose a "flavor alignment ansatz", introduced in Ref. [38], which postulates that the independent matrix Yukawa couplings are proportional to the corresponding quark and charged lepton mass matrices. In this case one finds that, in the mass basis for the quarks and leptons, the matrix Yukawa couplings are flavor diagonal, and the Higgs-mediated tree-level FCNCs are absent. One way to achieve alignment in the Yukawa sector is to introduce a set of discrete symmetries which constrain the Higgs scalar potential and Yukawa couplings. The so-called type-I and II 2HDMs [40], and the related type X and type Y 2HDMs [41,42] provide examples of this type. Indeed, Ref. [43] showed that the flavor alignment is preserved under RGE running if and only if such discrete symmetries are present. The flavor alignment ansatz is more general, but requires fine-tuning in the absence of an underlying symmetry.

This paper is organized as follows: In Sec. II, we review the basis-independent formalism as applied to the 2HDM. In Sec. III, we describe the Yukawa sector and present the flavor alignment model used in this analysis. In Sec. IV, we present our numerical analysis of the mass bounds governing the lightest scalar, which are derived by requiring the stability of the 2HDM potential and the absence of Landau poles in the scalar quartic couplings below the Planck scale. Our analysis employs both the one-loop RG running of the quartic couplings, along with an estimate of the effects of the two-loop corrections. In Sec. VI, we present our

conclusions. The one-loop basis independent RGEs are presented in Appendix A, and stability conditions on the basis-independent 2HDM potential are derived in Appendix B.

II. BASIS-INDEPENDENT TREATMENT OF THE 2HDM

A. The Higgs basis

In a generic basis, the most general renormalizable $SU(3)_C \times SU(2)_L \times U(1)_Y$ gauge-invariant 2HDM scalar potential is given by

$$
\begin{aligned}
\mathcal{V} &= m_{11}^2 (\Phi_1^\dagger \Phi_1) + m_{22}^2 (\Phi_2^\dagger \Phi_2) - [m_{12}^2 \Phi_1^\dagger \Phi_2 + \text{H.c.}] \\
&+ \frac{1}{2} \lambda_1 (\Phi_1^\dagger \Phi_1)^2 + \frac{1}{2} \lambda_2 (\Phi_2^\dagger \Phi_2)^2 + \lambda_3 (\Phi_1^\dagger \Phi_1)(\Phi_2^\dagger \Phi_2) \\
&+ \lambda_4 (\Phi_1^\dagger \Phi_2)(\Phi_2^\dagger \Phi_1) + \left\{ \frac{1}{2} \lambda_5 (\Phi_1^\dagger \Phi_2)^2 \right. \\
&\left. + [\lambda_6 (\Phi_1^\dagger \Phi_1) + \lambda_7 (\Phi_2^\dagger \Phi_2)](\Phi_1^\dagger \Phi_2) + \text{H.c.} \right\},
\end{aligned}
\tag{1}
$$

where Φ_1, Φ_2 are two hypercharge-one complex scalar doublets. The two doublets separately acquire vacuum expectation values (VEVs) $\langle \Phi_1^0 \rangle = v_1/\sqrt{2}$ and $\langle \Phi_2^0 \rangle = v_2/\sqrt{2}$ with the constraint $v^2 = |v_1|^2 + |v_2|^2 \simeq (246\,\text{GeV})^2$. The parameters $\lambda_{1,2,3,4}$ and m_{11}^2, m_{22}^2 are real whereas $\lambda_{5,6,7}$ and m_{12}^2 are potentially complex. The 2HDM is CP-conserving if there exists a basis in which all of the parameters and the vacuum expectation values are simultaneously real.

We shall adopt a basis-independent formalism as developed in Ref. [39], which provides basis-independent 2HDM potential parameters that are invariant under a global U(2) transformation of the two scalar doublet fields, $\Phi_a \to U_{a\bar{b}} \Phi_b$ ($a, \bar{b} = 1, 2$).

It is convenient to define the so-called *Higgs basis* of scalar doublet fields,

$$
\begin{aligned}
H_1 &= \begin{pmatrix} H_1^+ \\ H_1^0 \end{pmatrix} \equiv \frac{v_1^* \Phi_1 + v_2^* \Phi_2}{v}, \\
H_2 &= \begin{pmatrix} H_2^+ \\ H_2^0 \end{pmatrix} \equiv \frac{-v_2 \Phi_1 + v_1 \Phi_2}{v},
\end{aligned}
\tag{2}
$$

so that $\langle H_1^0 \rangle = v/\sqrt{2}$ and $\langle H_2^0 \rangle = 0$. The Higgs basis is uniquely defined up to a rephasing of the H_2 field, $H_2 \to e^{i\chi} H_2$. In the Higgs basis, the scalar potential takes the familiar form,[2]

$$
\begin{aligned}
\mathcal{V} &= Y_1 (H_1^\dagger H_1) + Y_2 (H_2^\dagger H_2) + [Y_3 H_1^\dagger H_2 + \text{H.c.}] \\
&+ \frac{1}{2} Z_1 (H_1^\dagger H_1)^2 + \frac{1}{2} Z_2 (H_2^\dagger H_2)^2 + Z_3 (H_1^\dagger H_1)(H_2^\dagger H_2) \\
&+ Z_4 (H_1^\dagger H_2)(H_2^\dagger H_1) + \left\{ \frac{1}{2} Z_5 (H_1^\dagger H_2)^2 \right. \\
&\left. + [Z_6 (H_1^\dagger H_1) + Z_7 (H_2^\dagger H_2)](H_1^\dagger H_2) + \text{H.c.} \right\},
\end{aligned}
\tag{3}
$$

where Y_1, Y_2, and $Z_{1,2,3,4}$ are real parameters and uniquely defined, whereas Y_3 and $Z_{5,6,7}$ transform under a rephasing of H_2, viz., $[Y_3, Z_6, Z_7] \to e^{-i\chi}[Y_3, z_6, Z_7]$ and $Z_5 \to e^{-2i\chi} Z_5$. Minimizing the scalar potential then yields

$$
Y_1 = -\frac{1}{2} Z_1 v^2, \qquad Y_3 = -\frac{1}{2} Z_6 v^2.
\tag{4}
$$

The scalar potential is CP-violating if no choice of χ can be found in which all Higgs basis scalar potential parameters are simultaneously real.

The tree-level mass eigenstates of the neutral scalars can be obtained by diagonalizing the neutral scalar squared-mass matrix in the Higgs basis [44,45],

$$
\mathcal{M} = v^2 \begin{pmatrix}
Z_1 & \text{Re}(Z_6) & -\text{Im}(Z_6) \\
\text{Re}(Z_6) & \frac{1}{2}[Z_3 + Z_4 + \text{Re}(Z_5)] + Y_2/v^2 & -\frac{1}{2}\text{Im}(Z_5) \\
-\text{Im}(Z_6) & -\frac{1}{2}\text{Im}(Z_5) & \frac{1}{2}[Z_3 + Z_4 - \text{Re}(Z_5)] + Y_2/v^2
\end{pmatrix}.
\tag{5}
$$

The diagonalizing matrix is a real orthogonal 3×3 matrix that is parameterized by three mixing angles θ_{12}, θ_{13}, and θ_{23} (details can be found in Ref. [45]). In terms of U(2)-invariant combinations of the mixing angles

---

[2] As discussed in Appendix A, the squared-mass and coupling coefficients, Y_1, Y_2, and $Z_{1,2,3,4}$ can be expressed as U(2)-invariant combinations of the scalar potential coefficients and the VEVs, whereas Y_3 and $Z_{5,6,7}$ are U(2)-pseudoinvariant combinations of the scalar potential coefficients and the VEVs that are rephased under a U(2) transformation [39].

and scalar potential parameters, the squared-masses of the three neutral Higgs bosons, denoted by h_1, h_2 and h_3, respectively, are given by [45]

$$
\begin{aligned}
m_k^2 &= |q_{k2}|^2 Y_2 + v^2 \left\{ q_{k1}^2 Z_1 + \frac{1}{2} |q_{k2}|^2 [Z_3 + Z_4 \right. \\
&- \text{Re}(Z_5 e^{-2i\theta_{23}})] + \text{Re}(q_{k2})\text{Re}(q_{k2} Z_5 e^{-2i\theta_{23}}) \\
&\left. + 2q_{k1}\text{Re}(q_{k2} Z_6 e^{-i\theta_{23}}) \right\}, \quad \text{for } k = 1, 2, 3,
\end{aligned}
\tag{6}
$$

TABLE I. q_{ki} as a function of the neutral Higgs mixing angles in the Higgs basis.

k	q_{k1}	q_{k2}
1	$\cos\theta_{12}\cos\theta_{13}$	$-\sin\theta_{12}-i\cos\theta_{12}\sin\theta_{13}$
2	$\sin\theta_{12}\cos\theta_{13}$	$\cos\theta_{12}-i\sin\theta_{12}\sin\theta_{13}$
3	$\sin\theta_{13}$	$i\cos\theta_{13}$

where the q_{ki} are invariant combinations of the mixing angles shown in Table I. It is convenient to choose a convention where $m_1 < m_2 < m_3$ (which can always be arranged by an appropriate choice of neutral Higgs mixing angles). The squared-mass of the charged scalars is given by

$$m_{H^\pm}^2 = Y_2 + \frac{1}{2}Z_3 v^2. \qquad (7)$$

B. Decoupling limit

The decoupling limit corresponds to taking the squared-mass parameter of the Higgs basis field H_2 large while holding the Higgs quartic coupling parameters fixed. In the perturbative regime, we take $|Z_i| \lesssim \mathcal{O}(1)$ and $Y_2 \gg v^2$. In this case [37,45],

$$\sin\theta_{12} \sim \sin\theta_{13} \sim \mathcal{O}\left(\frac{v^2}{Y_2}\right). \qquad (8)$$

In addition, the decoupling limit requires that

$$\mathrm{Im}(Z_5 e^{-2i\theta_{23}}) \sim \mathcal{O}\left(\frac{v^2}{Y_2}\right), \qquad (9)$$

which implies that

$$\mathrm{Re}(Z_5 e^{-2i\theta_{23}}) = -|Z_5|. \qquad (10)$$

The overall sign in Eq. (10) [which is not determined by Eq. (9)] is fixed in the convention where $m_2 < m_3$. Using the above results in Eq. (6) yields

$$m_1^2 = Z_1 v^2 \left[1 + \mathcal{O}\left(\frac{v^2}{Y_2}\right)\right], \qquad (11)$$

$$m_2^2 = Y_2 + \frac{1}{2}v^2 \left[Z_3 + Z_4 - |Z_5| + \mathcal{O}\left(\frac{v^2}{Y_2}\right)\right], \qquad (12)$$

$$m_3^2 = Y_2 + \frac{1}{2}v^2 \left[Z_3 + Z_4 + |Z_5| + \mathcal{O}\left(\frac{v^2}{Y_2}\right)\right]. \qquad (13)$$

At energy scales below Y_2, the effective low-energy theory corresponds to the Standard Model with one Higgs doublet. Consequently, in the decoupling limit the properties of h_1 approach those of the SM Higgs boson. The nonminimal Higgs states are roughly degenerate in mass, $m_2^2 \sim m_3^2 \sim m_{H^\pm}^2 \sim Y_2$, with squared-mass splittings of $\mathcal{O}(v^2)$,

$$m_3^2 - m_2^2 \simeq |Z_5| v^2, \qquad (14)$$

$$m_3^2 - m_{H^\pm}^2 \simeq \frac{1}{2}(Z_4 + |Z_5|) v^2. \qquad (15)$$

In the decoupling limit of a general 2HDM, the tree-level CP-violating and flavor-changing neutral Higgs couplings of the SM-like Higgs state h_1 are suppressed by factors of $\mathcal{O}(v^2/Y_2^2)$. The corresponding interactions of the heavy neutral Higgs bosons (h_2 and h_3) and the charged Higgs bosons ($H^\pm$) can exhibit both CP-violating and flavor nondiagonal couplings. If Y_2 is sufficiently large, then FCNCs mediated by the lightest neutral scalar can be small enough to be consistent with experimental data. However, for values of Y_2 of order 1 TeV and below, tree-level Higgs-mediated FCNCs are problematical in the case of a generic Yukawa sector.

III. YUKAWA SECTOR

The most general 2HDM Yukawa sector, describing Higgs-fermion interactions, includes six Yukawa matrices (as compared to three in the SM). In a generic basis, the Yukawa Lagrangian for the Higgs-quark interactions is given by Eq. (A1). Following the discussion of Appendix A, we can reexpress the Yukawa Lagrangian in terms of the quark mass-eigenstate fields [46],

$$
\begin{aligned}
-\mathcal{L}_Y = {} & \bar{U}_L(\eta_1^U \Phi_1^{0*} + \eta_2^U \Phi_2^{0*}) - \bar{D}_L K^\dagger(\eta_1^U \Phi_1^- + \eta_2^U \Phi_2^-)U^R \\
& + \bar{U}_L K(\eta_1^{D\dagger}\Phi_1^+ + \eta_2^{D\dagger}\Phi_2^+)D^R \\
& + \bar{D}_L(\eta_1^{D\dagger}\Phi_1^0 + \eta_2^{D\dagger}\Phi_2^0)D^R + \mathrm{H.c.},
\end{aligned} \qquad (16)
$$

where $\eta_{1,2}^{U,D}$ are 3×3 Yukawa coupling matrices and K is the CKM matrix.

Using Eq. (2), one can rewrite Eq. (16) in terms of the Higgs basis scalar doublet fields,

$$
\begin{aligned}
-\mathcal{L}_Y = {} & \bar{U}_L(\kappa^U H_1^{0\dagger} + \rho^U H_2^{0\dagger})U^R - \bar{D}_L K^\dagger(\kappa^U H_1^- + \rho^U H_2^-)U^R \\
& + \bar{U}_L K(\kappa^{D\dagger}H_1^+ + \rho^{D\dagger}H_2^+)D^R \\
& + \bar{D}_L(\kappa^{D\dagger}H_1^0 + \rho^{D\dagger}H_2^0)D^R + \mathrm{H.c.},
\end{aligned} \qquad (17)
$$

where[3]

$$\kappa^Q \equiv \frac{v_1^*\eta_1^Q + v_2^*\eta_2^Q}{v}, \qquad \rho^Q \equiv \frac{-v_2\eta_1^Q + v_1\eta_2^Q}{v}. \qquad (18)$$

Note that $\rho^Q \to e^{-i\chi}\rho^Q$ with respect to the rephasing $H_2 \to e^{i\chi}H_2$. Since $\langle H_1^0 \rangle = v/\sqrt{2}$ and $\langle H_2^0 \rangle = 0$, it follows that the $\kappa^{U,D}$ are proportional to the diagonal quark mass matrices, M_U and M_D, whose matrix elements are real and non-negative,

---

[3]As noted in Eq. (A6), the ρ^Q are U(2)-pseudoinvariant combinations of the Yukawa coupling matrices and the VEVs, whereas the κ^Q are U(2) invariants.

$$M_U = \frac{v\kappa^U}{\sqrt{2}} = \mathrm{diag}(m_u, m_c, m_t),$$

$$M_D = \frac{v\kappa^D}{\sqrt{2}} = \mathrm{diag}(m_d, m_s, m_b). \tag{19}$$

The Yukawa couplings of the Higgs doublets to the leptons can be similarly treated by replacing $U \to N$, $D \to E$, $M_U \to 0$, $M_D \to M_E$ and $K \to \mathbb{1}$, where $N = (\mu_e, \nu_\mu, \nu_\tau)$, $E = (e, \mu, \tau)$ and M_E is the diagonal charged lepton mass matrix.

Since the Yukawa matrices $\rho^{U,D,E}$ are independent complex 3×3 matrices, it follows that the Yukawa Lagrangian exhibited in Eq. (17) generically exhibits tree-level Higgs mediated FCNCs. The off-diagonal elements of the $\rho^{U,D}$ matrices are highly constrained by experimental data to be very small. As first shown by Glashow, Weinberg and Paschos (GWP) [47,48], it is possible to *naturally* eliminate tree-level Higgs mediated FCNCs if, for some choice of basis of the scalar fields, at most one Higgs multiplet is responsible for providing mass for quarks or leptons of a given electric charge. In the 2HDM, the GWP condition is usually imposed in four different ways by employing the appropriate $\mathbb{Z}_2$ discrete symmetry [40–42,49,50]:

 (1) Type-I Yukawa couplings: $\eta_1^U = \eta_1^D = \eta_1^L = 0$,
 (2) Type-II Yukawa couplings: $\eta_1^U = \eta_2^D = \eta_2^L = 0$.
 (3) Type-X Yukawa couplings: $\eta_1^U = \eta_1^D = \eta_2^L = 0$,
 (4) Type-Y Yukawa couplings: $\eta_1^U = \eta_2^D = \eta_1^L = 0$.

For example, it follows from Eq. (18) that in the type-I 2HDM,

$$\rho^{U,D,L} = \frac{v_1}{v_2^*} \kappa^{U,D,L}, \tag{20}$$

and in the type-II 2HDM,

$$\rho^U = \frac{v_1}{v_2^*} \kappa^U,$$

$$\rho^{D,L} = -\frac{v_2}{v_1^*} \kappa^{D,L}. \tag{21}$$

In light of Eq. (19), the ρ^F $(F = U, D, L)$ are, in these cases, diagonal matrices in which case the neutral Higgs–fermion Yukawa interactions are flavor-diagonal at tree-level.

If only phenomenological considerations are invoked in choosing the Higgs–fermion Yukawa couplings, then it is possible to consider the more general case of the flavor-aligned 2HDM introduced in Ref. [38]. In this model applied to the Higgs basis, one imposes the following conditions

$$\rho^U = \alpha^U \kappa^U, \qquad \rho^D = \alpha^D \kappa^D, \quad \text{and} \quad \rho^L = \alpha^L \kappa^L, \tag{22}$$

which generalize the type-I and II results exhibited in Eqs. (20) and (21). In Eq. (22), the alignment parameters,

$\alpha^{U,D,L}$, are arbitrary complex constants.[4] The flavor alignment condition shown in Eq. (22) is not imposed by any symmetry, and is strictly unnatural (i.e., it can be achieved only by a fine-tuning of the model parameters). Equivalently, as observed in Ref. [43], the flavor alignment is preserved under RGE running only in the case of type I, II, X and Y Yukawa couplings. Nevertheless, one can imagine the possibility of new dynamics above the electroweak scale that could be responsible for an approximately flavor-aligned 2HDM. Thus, in our analysis we shall employ the more general Eq. (22), which is sufficient for satisfying the phenomenological FCNC constraints.[5]

IV. RG STABILITY AND PERTURBATIVITY OF THE 2HDM

Let us assume that the observed SM-like Higgs boson (with $m_h \simeq 125$ GeV) is part of a 2HDM in the decoupling limit with a flavor-aligned Yukawa sector, with no other new physics present beyond the 2HDM below the Planck scale.[6] We shall examine whether there are regions of the 2HDM parameter space that yield a consistent model under RG running from the electroweak to the Planck scale. In general, two potential problems can arise in the RG evolution. First, Landau poles could arise from the divergence of the 2HDM quartic scalar couplings and/or Yukawa couplings. Second, the 2HDM scalar potential could become unstable at a higher energy scale. The case of Landau poles is fairly straightforward, although the precise energy scale at which they arise cannot be strictly determined, since it lies outside the perturbative regime of the RGEs. In practice, we shall consider that a Landau pole occurs when the relevant coupling exceeds 100 for some energy scale $\Lambda \leq M_{Pl}$. Indeed, once such a large coupling is reached, it will very quickly diverge at an energy scale very close to Λ. In our analysis, we employ the one-loop RGEs for the quartic scalar couplings of the 2HDM in the Higgs basis given in Appendix A. These equations are strongly coupled, and thus a divergence in one quartic scalar coupling will cause a divergence in the rest. The leading effects of two-loop running will be assessed at the end of this section.

---

[4]In practice, if the magnitude of the alignment constants are too large, then some of the Higgs-fermion Yukawa couplings will develop Landau poles below the Planck scale. In our analysis, we will determine the allowed regions of the flavor-aligned 2HDM parameter space where such Landau poles are absent.

[5]By choosing to work in the decoupling limit where $Y_2 \gtrsim (500 \text{ GeV})^2$, we ensure that FCNCs generated by one-loop radiative effects are not too large to be in conflict with experimental data (see e.g. Ref. [51]).

[6]Incorporating light neutrino masses via the seesaw mechanism [52] with the mass scale of the right-handed neutrino sector assumed to be of order a typical grand unified scale has a very minor impact on the considerations in this paper.

In the SM, the requirement that the scalar potential is stable at all energy scales below the scale Λ is easily implemented. It is sufficient to require that the SM quartic scalar coupling is positive, i.e. $\lambda_{\mathrm{SM}}(\Lambda) > 0$ for $\Lambda > v$. Requiring that the 2HDM scalar potential is stable at all energy scales below the scale Λ leads to a more complicated set of conditions. In the 2HDM with an unbroken, or softly broken, $\mathbb{Z}_2$ discrete symmetry that sets $\lambda_6 = \lambda_7 = 0$ in Eq. (1), the stability conditions were first obtained in Ref. [53],

$$\lambda_1 > 0, \tag{23}$$

$$\lambda_2 > 0, \tag{24}$$

$$\lambda_3 > -\sqrt{\lambda_1 \lambda_2}, \tag{25}$$

$$\lambda_3 + \lambda_4 - |\lambda_5| > -\sqrt{\lambda_1 \lambda_2}. \tag{26}$$

However, in the case of a completely general scalar potential, the corresponding stability conditions are far more complicated (with no simple analytic form). Reference [54] provides an algorithm for deriving the stability conditions for a general 2HDM, with no symmetry or CP assumptions imposed on the 2HDM scalar potential. In terms of the Higgs basis parameters, this algorithm is summarized in Appendix B. Except for special cases for the quartic scalar couplings, the corresponding stability conditions must be determined numerically.

We now describe in detail the procedure used in our analysis. We assume that we are in the decoupling regime of the 2HDM, where the mass scale of the heavy Higgs sector is of $\mathcal{O}(\Lambda_H)$. In light of Eqs. (7), (12) and (13), we henceforth set $\Lambda_H^2 \equiv Y_2$.

(1) Start with the SM Higgs potential defined at the scale of the 125 GeV Higgs boson.

(2) Use SM RG evolution to run the Higgs-self coupling parameter λ and the fermion mass matrices up to the scale Λ_H.[7]

(3) Match the one-doublet Higgs potential with the 2HDM potential by taking $Z_1 = \lambda(\Lambda_H)$ and $\kappa^F = \sqrt{2} M_F(\Lambda_H)/v$ (for $F = U, D$). This establishes the low energy boundary conditions. The effects of the lepton masses are negligible and have been ignored.

(4) Scan over all other 2HDM quartic scalar coupling parameters Z_i and Yukawa alignment parameters α^F ($F = U, D$). The latter fix the values of the $\rho^F(\Lambda_H)$.

(5) Run the 2HDM RGEs for the Z_i, κ^F and ρ^F up to higher energies Λ. Check for stability of the potential at the scale Λ using the procedure summarized in Appendix B.

(6) Stop the running if a Landau pole is encountered or if the stability conditions cannot be satisfied.

For the scalar sector, we scanned over the parameter space using 100,000 points, with $|Z_i| \lesssim \mathcal{O}(1)$, for $i = 2, ..., 7$, to enforce the decoupling limit. These points were also subject to the constraint that they obey the stability conditions presented in Appendix B. Note that when $|Z_i| \ll 1$ for $i = 2, ..., 7$, we recover the SM Higgs sector. The choice of Λ_H is subject to the condition $\Lambda_H^2 \gg v^2$, so that we are safely in the decoupling regime. Moreover, in order for the 2HDM to be distinguishable from the SM Higgs sector, Λ_H should not be significantly larger than $\mathcal{O}(1\ \mathrm{TeV})$. We considered two different values, $\Lambda_H = 500$ GeV and 1 TeV, although the allowed parameter regime in which the 2HDM remains consistent up to the Planck scale is not especially sensitive to the precise value of Λ_H in the desired mass range. In the case of $\Lambda_H = 500$ GeV, it is plausible that the heavy Higgs boson states could be detected in high luminosity LHC running. Indeed, as we shall demonstrate later in this section, differences in the squared-masses of the heavy Higgs states can provide an important consistency check of this framework.

The Yukawa couplings play a fundamental role in this analysis. As discussed in Sec. III, we have employed the flavor aligned 2HDM to describe the Yukawa sector, with random complex alignment parameters whose moduli were varied by several orders of magnitude. The evolution of the Yukawa couplings in the flavor-aligned 2HDM was first performed in Ref. [57]. Notice that the running of the Yukawa couplings can also generate Landau poles. Due to the large size of the top quark mass, at least one of the Yukawa couplings will be of order one at the electroweak scale, so that a Landau pole in the top-quark Yukawa coupling below the Planck scale can be generated by the RG running. The alignment parameters, unique for both the up and down quark sectors, were log random generated in such a way as to prevent such Landau poles in the running of the Yukawa couplings up to Planck scale. In the RG running, the initial value of the top Yukawa coupling was taken to be $y_t(m_t) = 0.94$, corresponding to an $\overline{\mathrm{MS}}$ top quark mass of $m_t(m_t) = 163.71 \pm 0.9$ GeV [56]. The non-occurrence of Landau poles then leads to the constraints[8]

$$|\alpha^U| \lesssim 0.95 \quad \text{and} \quad |\alpha^D| \lesssim 81.5, \tag{27}$$

as seen in Fig. 1. These results are quite consistent with those obtained in Ref. [57].

The effect of the alignment parameters in the one-loop quartic scalar coupling RGEs is to bolster the negative

---

[7]Starting the RG evolution at m_Z, we use a five flavor scheme to run up to m_t and a six flavor scheme above m_t. Running quark mass masses at m_Z and m_t are obtained from the RUNDEC MATHEMATICA software package [55], based on quark masses provided in Ref. [56]. For simplicity, the effects of the lepton masses are ignored, as these contribute very little to the running of the Z_i.

[8]For $\Lambda_H = 1$ TeV, we find $|\alpha^U| \lesssim 0.97$ and $|\alpha^D| \lesssim 84$. The figure corresponding to Fig. 1 looks nearly identical, so we do not display it here.
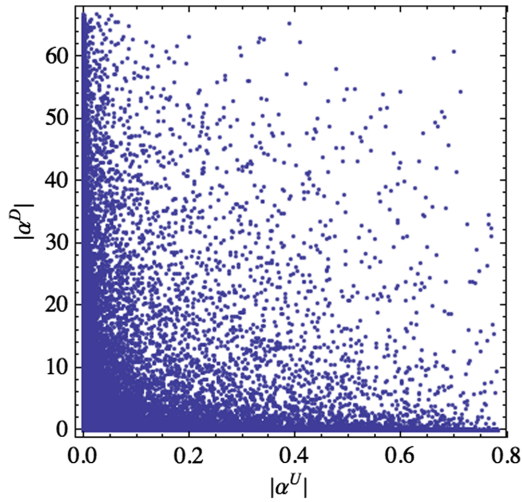
FIG. 1 (color online). Distribution of absolute values of the flavor alignment parameters, for regions of 2HDM parameter space which remain valid up to the Planck scale, assuming $\Lambda_H = 500$ GeV.

Yukawa terms, thereby further driving the quartic scalar couplings to be negative during RGE evolution. The influence of the Yukawa couplings in the scalar couplings RG evolution is dominated by y_t^4 terms (where y_t is the top quark Yukawa coupling) in the one-loop β functions, where they provide a negative contribution. In this manner, the large size of the top quark Yukawa coupling tends to drive Z_1 negative at large energy scales, thus provoking an instability in the potential. This will occur unless the starting point value (at the electroweak scale) of Z_1 is large enough. Since Z_1 is directly related to the lightest CP-even mass in the decoupling regime, requiring the stability of the scalar potential between the electroweak scale and the Planck one therefore yields a lower bound on m_h. Similarly, if the initial value of Z_1 at the electroweak scale is too large, then a Landau pole will appear in the running of Z_1 below the Planck scale due to the fact that the leading Z_i contributions to the β functions of the quartic scalar couplings are positive, thereby driving the quartic scalar couplings to larger values as the energy scale increases. Preventing the occurrence of Landau poles thus establishes an upper bound on Z_1, and thus on m_h.

Within the SM, these demands can only be satisfied up to the Planck scale by a rather narrow window of Higgs boson masses, which excludes the observed value of 125 GeV. As we shall now see, the complexity of the 2HDM scalar potential "opens up" that narrow window to include the known value of the Higgs mass.

V. NUMERICAL ANALYSIS

A. Results from one-loop RG running

Let us now compare the effect of the one-loop running of the SM scalar coupling, with its effect on the 2HDM quartic scalar couplings. The results of our calculations are shown
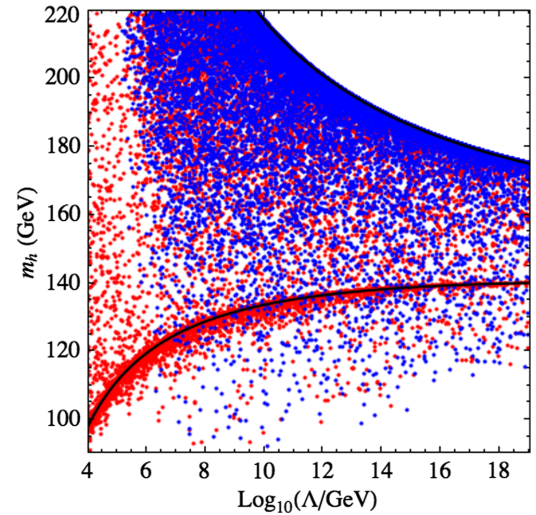

FIG. 2 (color online). RG running of 2HDM quartic scalar couplings, with $\Lambda_H = 1$ TeV. Red points correspond to parameter choices for which an instability occurs in the scalar potential; blue points indicate the presence of a Landau pole. The upper solid black line indicates the occurrence of a Landau pole in the SM. The lower solid black line indicates the limit for which the SM potential becomes unstable.

in Fig. 2, which we now analyze in detail. The full 2HDM running begins at $\Lambda_H = 1$ TeV, where the Z_i for $i = 2,\ldots,7$ are chosen.[9] The red points in Fig. 2 correspond to choices of parameters Z_i for which an instability of the potential occurred for a given higher scale $\Lambda > \Lambda_H$. The blue points correspond to parameter choices for which a Landau pole occurred during the RG running at some scale $\Lambda > \Lambda_H$. These results are to be compared with the corresponding results of the SM Higgs sector also shown in Fig. 2: the upper solid line indicates the maximally allowed value of m_h to avoid a Landau pole and the lower solid line indicates the minimal value of m_h needed to avoid a negative SM quartic scalar coupling, at all energy scales below Λ. We recover the well-known one-loop SM result that $140 \lesssim m_h \lesssim 175$ GeV in order to preserve vacuum stability and avoid Landau poles in the running of the quartic scalar coupling at all energy scales up to $M_{\rm PL}$ [5–12].

The distribution of red and blue points in Fig. 2 has some interesting features. First, there are no blue points above the SM-Landau pole line. In fact, although the 2HDM scalar potential has several scalar couplings, their contributions to the 2HDM β functions are mostly positive. As such, when one of these couplings starts to become very large in its RG evolution, the others will not be able to counteract that growth, and a Landau pole is reached. Consequently, the upper limit for the quartic scalar coupling Z_1 that controls the value of m_h hardly differs from the corresponding SM result. Second, note the appearance of many blue points

---

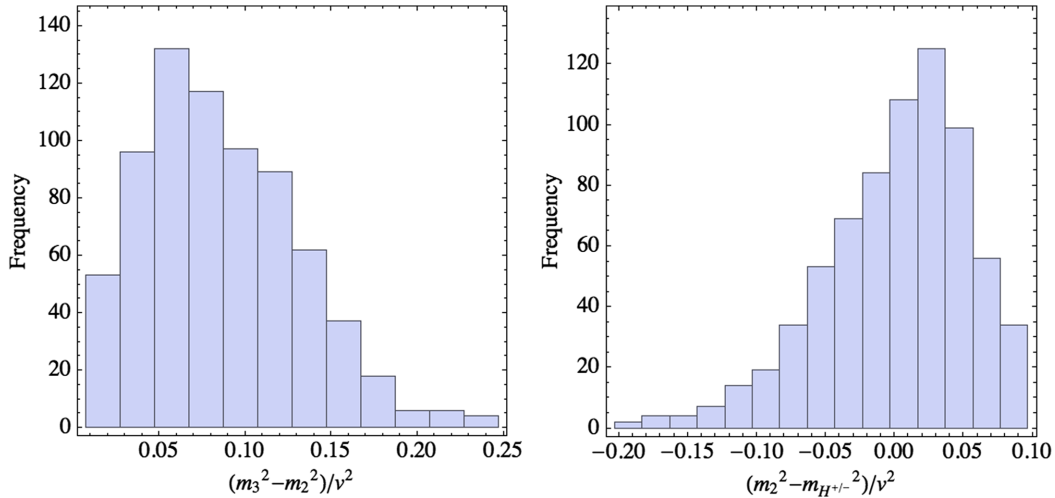[9]The corresponding plot for $\Lambda_H = 500$ GeV looks nearly identical, so we do not exhibit it here.

FIG. 3 (color online).   Histograms of squared-mass differences of the heavy scalar states for $\Lambda_H = 500$ GeV. The left panel shows values of squared-mass difference between the two heavier neutral states. The right panel shows the values of the squared-mass difference between the lighter of the two heavy neutral states and the charged Higgs boson. The histograms correspond to 2HDM parameters for which there are no Landau poles and vacuum stability is satisfied at all energies below the Planck scale.

below the SM-instability line. These correspond to Landau poles that occur for relatively low values of m_h, which is equivalent to low values of Z_1. However, even though the initial value of Z_1 at Λ_H may be small, the values of other Z_i can be large, and thus Landau poles in these couplings can be generated, yielding those blue points below the SM instability line.

The most interesting aspect of our results concerns the distribution of the red points, which correspond to the violation of one or more of the 2HDM stability conditions at the energy scale Λ. We see a great "density" of points around the SM-instability line. These points may be interpreted as regions of 2HDM parameter space that constitute small deviations from SM behavior. But the remarkable difference with the SM result is the appearance of many points *below and to the right* of the SM-instability line. For these points, the instability of the scalar potential occurs at a larger value of Λ for a given value of m_h as compared to the SM. Indeed, the full impact of the 2HDM on the RG evolution may be best appreciated by examining the rightmost boundary of Fig. 2 corresponding to $\Lambda = M_{PL}$. On this boundary, we find both blue and red points, for a range of Higgs masses from about 118 GeV up to 175 GeV. Thus we see that a range of 2HDM parameters exists for which it is possible to have a SM-like Higgs boson with a mass of 125 GeV, without that mass value implying an instability of the potential (or a Landau pole) between the electroweak and Planck scales.

Let us now analyze more closely the region of parameter space for which the 2HDM is consistent up to the Planck scale. According to Fig. 2, only a narrow range of m_h (which corresponds to a narrow interval of values of Z_1) is consistent with a 2HDM with a stable vacuum and no Landau poles from the electroweak to the Planck scale.

Since the 2HDM quartic couplings are all coupled together in their RG running, it follows that the allowed ranges for all Z_i, not only Z_1, will likewise be quite narrow. This has interesting implications on the scalar mass spectrum. In fact, in light of Eq. (14), the squared-mass splitting of the two heavy neutral Higgs states depends primarily on $|Z_5|$. Likewise, Eq. (15) shows that the squared-mass splitting of the heavier neutral Higgs boson and the charged Higgs boson primarily depends on Z_4 and $|Z_5|$. Since the possible values of Z_4 and $|Z_5|$ are restricted to a narrow range of values, it follows that the squared-mass splittings of the heavy Higgs states should also be strongly constrained.

For a 125 GeV SM-like Higgs boson, we have evaluated the squared-mass splittings of the heavier Higgs bosons for 2HDM parameters that are consistent with a stable scalar potential and an absence of Landau poles up to the Planck scale. The histograms shown in Fig. 3 exhibit the distributions in arbitrary units of the squared-mass difference between the two heavy neutral states (which is positive by definition) and the difference between the lighter of the two heavy neutral states and the charged Higgs pair, for $\Lambda_H = 500$ GeV. Given the formulas in Sec. IIB, all the heavy scalars have masses of order Λ_H in the decoupling limit. The statistics of these histograms are summarized in Table II. If the 2HDM is valid up to the Planck scale, then the mass differences among the heavy Higgs states must be quite small. This presents a challenge for heavy Higgs searches at future colliders. It may be that such a spectrum could only be reliably determined at a multi-TeV lepton collider. Indeed, if the heavy Higgs spectrum could be determined at some future collider, it would provide a nontrivial check of the present framework in which the 2HDM is valid up to the Planck scale.

TABLE II. Squared mass splittings of the heavier Higgs bosons of the 2HDM with $\Lambda_H = 500$ GeV, for $124 \lesssim m_h \lesssim 126$ GeV, for points that survive up to the Planck scale, using one-loop calculations.

	Min	Max	Mean	Std. dev.
$(m_3^2 - m_2^2)/v^2$	0.01	0.26	0.09	0.05
$(m_2^2 - m_{H^\pm}^2)/v^2$	−0.20	0.11	0	0.05
$(m_3^2 - m_{H^\pm}^2)/v^2$	−0.07	0.19	0.09	0.04

TABLE III. Squared mass splittings of the heavier Higgs bosons of the 2HDM with $\Lambda_H = 1$ TeV, for $124 \lesssim m_h \lesssim 126$ GeV, for points that survive up to the Planck scale, using one-loop calculations.

	Min	Max	Mean	Std. dev.
$(m_3^2 - m_2^2)/v^2$	0	0.29	0.09	0.05
$(m_2^2 - m_{H^\pm}^2)/v^2$	−0.23	0.12	0	0.06
$(m_3^2 - m_{H^\pm}^2)/v^2$	−0.08	0.19	0.09	0.04

The results shown in Table II are not particularly sensitive to the value of Λ_H. For example, if $\Lambda_H = 1$ TeV, then the distribution of possible squared-mass differences yields the results shown in Table III. Of course, in this case the corresponding mass differences are even smaller, and the separate discovery of each of these new scalar states at a future collider is even more challenging.

B. The effects of two-loops RG running

In the SM, the inclusion of the two-loop terms in the RGEs shifts the scalar potential instability boundary to a higher energy scale, which lowers the minimum Higgs boson mass that is consistent with a stable scalar potential all the way up to the Planck scale. In particular, the results in Ref. [14] yield a minimal value of $m_h \simeq 129$ GeV for vacuum stability. Moreover, given the currently observed value of 125 GeV for the Higgs boson, the SM vacuum is metastable under the assumption of no new physics beyond the Standard Model below about 10^{10} GeV. This means that the effect of including two-loop effects in the RG running lowers by about 10 GeV the minimal value of the Higgs mass that is consistent with vacuum stability.

We expect that employing the full two-loop RG analysis for the 2HDM would provide a similar downward shift in the lower bound of Higgs masses that survive up to the Planck scale, as well as increase the fraction of points that survive. In practice, implementing this full two-loop procedure is computationally expensive. Instead, we present a procedure to estimate the two-loop RG results. Note that the stability curve for the SM scalar potential at two-loops is both shifted to a higher energy scale, and is less steep as a function of the Higgs mass, relative to the one-loop SM scalar potential stability curve. In essence, going from one-loop to two-loops shifts the stability curve energy scale to a higher scale for a particular Higgs mass. From our one-loop SM calculations and the two-loop SM calculations of Ref. [14], we determine the energy scale shift of the SM scalar potential stability curves due to the inclusion of two-loop RG running. Taking $\Lambda_H = 1$ TeV, the resulting scale shift function is shown in the left panel of Fig. 4, which then yields our "two-loop" result shown in the right panel, which is obtained by applying the scale shift to our one-loop calculation. This shift is applied only to those points in which the scalar potential became unstable, not for points that hit a Landau pole before the Planck scale.
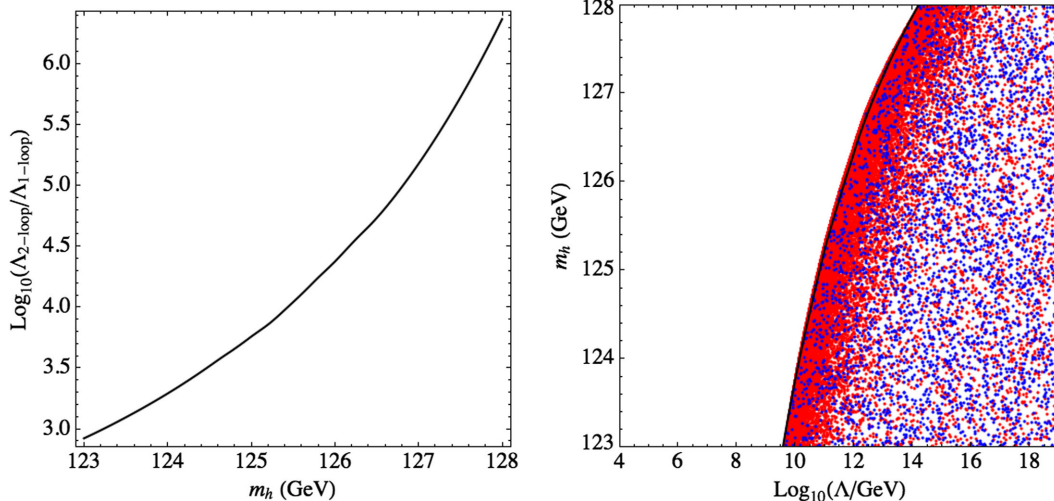

FIG. 4 (color online).   Left panel: Scale shift for converting the one-loop scalar potential instability boundary to the two-loop scalar potential instability boundary for a SM-like Higgs boson. Right panel: Higgs boson mass bounds in the flavor-aligned 2HDM, incorporating the scale shift shown in the left panel, assuming that $\Lambda_H = 1$ TeV. Red points indicate an instability in the running; blue points indicate the presence of a Landau pole.

TABLE IV.   Squared-mass splittings of the heavy Higgs bosons of the 2HDM with $\Lambda_H = 1$ TeV, for $m_h \simeq 125$ GeV, for points that survive to the Planck scale, using the two-loop extended procedure.

	Min	Max	Mean	Std. dev.
$(m_3^2 - m_2^2)/v^2$	0	0.31	0.11	0.05
$(m_2^2 - m_{H^\pm}^2)/v^2$	-0.23	0.12	0	0.05
$(m_3^2 - m_{H^\pm}^2)/v^2$	-0.09	0.23	0.11	0.04

The upper bound on the SM Higgs mass due to the absence of Landau poles does not exhibit a similar shift from one-loop to two-loop calculations. As in the case of Fig. 2, the case of $\Lambda_H = 500$ GeV yields nearly identical results.

In our one-loop calculations, only 707 (or 0.707%) of the 100,000 points analyzed survive to the Planck scale in the 123 GeV to 128 GeV region. With the conversion shift and a double check that they satisfy the stability requirement for 2HDM quartic scalar coupling parameters, 1,371 more points reach the Planck scale for a total of 2,078 (or 2.078%) at the Planck scale, an increase of 94% relative to the one-loop results. With an increase in the number of points, the "two-loop" squared mass splittings of the heavier Higgs bosons for points that survive up to the Planck scale are given in Table IV. Comparing Tables III and IV, we see that there exists only slight differences in the squared-mass splittings of the heavier Higgs bosons when the approximate two-loop effects are included. Nonetheless, the increase in the number of points for which the model remains consistent all the way up to the Planck scale is according to what one should expect, in light of the observation that the two-loop contributions increase the stability of the SM potential. Thus, this quick estimate suggests that the 2HDM parameter space corresponding to a stable scalar potential and no Landau poles in the RG running to the Planck scale is somewhat larger than the parameter regime identified in the one-loop analysis. In particular, given the observed Higgs mass of the 125 GeV, there exists a robust region of the parameter space for which the validity of the 2HDM and the stability of the Higgs vacuum is preserved up to the Planck scale.

VI. CONCLUSIONS

The discovery of a SM-like Higgs boson with a mass $m_h = 125$ GeV has focused attention on the validity of the Standard Model at higher energies. Putting aside the question of the origin of the electroweak symmetry breaking (e.g., accepting the fine-tuning of parameters inherent in fixing the electroweak scale), one can ask whether the Standard Model is consistent all the way up to the Planck scale. Refined calculations of the radiatively-corrected scalar potential suggest that the Standard Model vacuum is at best metastable (and long-lived), with a deeper vacuum located at field values near 10^{10} GeV, well below the Planck scale.

Adding new degrees of freedom has the potential of ameliorating the problem of an unstable vacuum. In this paper we considered the two-Higgs-doublet extension of the Standard Model (2HDM) and examined the range of parameters for which the 2HDM is stable and perturbative at all energy scales below the Planck scale. Our aim was to make the minimal number of assumptions regarding the structure of the 2HDM required by the experimental data. Since the observed Higgs boson is SM-like (within the accuracy of the limited Higgs data set), we considered the 2HDM with the most general scalar potential in the decoupling regime. The Yukawa sector was treated using the flavor alignment ansatz, in which the second set of Yukawa matrices is proportional to the SM-like set at the electroweak scale to protect against tree-level Higgs-mediated FCNCs. Although the flavor alignment condition is not protected by a low-energy symmetry (except in special cases, which lead to 2HDMs of types I, II, X or Y), it provides a more general framework which at present is consistent with experimental data.

We scanned over the scalar potential parameters and the flavor alignment parameters to fix the boundary conditions at the scale of the heavy Higgs states. We then employed one-loop RGEs to run the 2HDM parameters up to the Planck scale, and required that no Landau poles are encountered, without generating an instability in the scalar potential. In contrast to the Standard Model, it is possible to have a SM-like Higgs boson with a mass of 125 GeV while maintaining the validity of the 2HDM up to the Planck scale. We also presented a scheme to estimate the effects of the RG-running at two-loops, by applying a scale shift seen in going from the one-loop SM scalar potential stability curve to the two-loop SM scalar potential stability curve. Such effects *increase* the number of points in the 2HDM parameter scan that survive Landau pole and stability requirements up to the Planck scale.

The larger range of allowed values of m_h in the 2HDM (as compared with the SM) is a direct consequence of the fact that the 2HDM scalar potential contains more quartic scalar couplings than the SM, which increases the stability of the potential at all scales between the electroweak and the Planck scale. In contrast, we observed that the theoretical upper bound on m_h in the 2HDM based on the nonexistence of Landau poles up to Planck scale hardly differs from the corresponding SM behavior. This can be understood as follows. In the SM, the negative top Yukawa contribution in the quartic scalar coupling β function drives that coupling to negative values during RG running, unless its starting point is sufficiently large. In the 2HDM, even if the initial values of *some* of the quartic scalar couplings are small, and even though the top quark contributions to the β functions are still negative, other couplings are allowed to have large values, which (in some cases) counterbalance

any putative instabilities arising due to RG running. The 2HDM scalar potential is thus comparatively more stable than that of the SM.

Finally, we have obtained bounds on the square-mass differences of the heavier Higgs bosons in the parameter regime where the 2HDM remains valid up to the Planck scale. If the 2HDM is realized in nature, this could provide an important check of the consistency of the model.

APPENDIX A: ONE-LOOP RENORMALIZATION GROUP EQUATIONS

The one-loop RGEs for the SM used in this analysis are provided by Ref. [58]. The 2HDM one-loop RGEs in various bases are given in Refs. [43,54,59–61]. The one-loop RGEs found in the literature typically assume a 2HDM scalar potential with a $\mathbb{Z}_2$ symmetry, $\Phi_1 \to \Phi_1$, $\Phi_2 \to -\Phi_2$, to avoid FCNCs and/or are explicitly CP-conserving. Here, we present one-loop RGEs for the full 2HDM, using a basis-independent approach and making no CP assumptions.

In a general 2HDM, the Higgs fermion interactions are governed by the following interaction Lagrangian:

$$-\mathcal{L}_{\mathrm{Y}} = \overline{Q_L^0} \tilde{\Phi}_a \eta_a^{U,0} U_R^0 + \bar{Q}_L^0 \Phi_a (\eta_{\bar{a}}^{D,0})^\dagger D_R^0 + \bar{E}_L^0 \Phi_a (\eta_{\bar{a}}^{E,0})^\dagger E_R^0 + \mathrm{H.c.}, \qquad (A1)$$

summed over $a, \bar{a} = 1, 2$, where $\Phi_{1,2}$ are the Higgs doublets, $\tilde{\Phi}_{\bar{a}} \equiv i\sigma_2 \Phi_{\bar{a}}^*$, Q_L^0 and E_L^0 are the weak isospin quark and lepton doublets, and U_R^0, D_R^0, E_R^0 are weak isospin quark and lepton singlets. [The right and left-handed fermion fields are defined as usual: $\psi_{R,L} \equiv P_{R,L}\psi$, where $P_{R,L} \equiv \frac{1}{2}(1 \pm \gamma_5)$.] Here, Q_L^0, E_L^0, U_R^0, D_R^0, E_R^0 denote the interaction basis states, which are vectors in the quark and lepton flavor spaces, and $\eta_1^{U,0}, \eta_2^{U,0}, \eta_1^{D,0}, \eta_2^{D,0}, \eta_1^{E,0}, \eta_2^{E,0}$ are 3×3 matrices in quark and lepton flavor spaces.

The neutral Higgs states acquire vacuum expectation values,

$$\langle \Phi_a^0 \rangle = \frac{v\hat{v}_a}{\sqrt{2}}, \qquad (A2)$$

where $\hat{v}_a \hat{v}_{\bar{a}}^* = 1$ and $v = 246$ GeV. It is also convenient to define

$$\hat{w}_b \equiv \hat{v}_{\bar{a}}^* \epsilon_{ab}, \qquad (A3)$$

where $\epsilon_{12} = -\epsilon_{21} = 1$ and $\epsilon_{11} = \epsilon_{22} = 0$.

It is convenient to define invariant and pseudoinvariant matrix Yukawa couplings [39,45],

$$\kappa^{F,0} \equiv \hat{v}_{\bar{a}}^* \eta_a^{F,0}, \qquad \rho^{F,0} \equiv \hat{w}_{\bar{a}}^* \eta_a^{F,0}, \qquad (A4)$$

where $F = U$, D or E. Inverting these equations yields

$$\eta_a^{F,0} = \kappa^{F,0} \hat{v}_a + \rho^{F,0} \hat{w}_a. \qquad (A5)$$

Note that under the U(2) transformation, $\Phi_a \to U_{a\bar{b}} \Phi_b$ [cf. Eq. (A35)],

$$\kappa^{F,0} \text{ is invariant and } \rho^{F,0} \to (\det U)\rho^{F,0}. \qquad (A6)$$

The Higgs fields in the Higgs basis are defined by [45]

$$H_1 \equiv \hat{v}_{\bar{a}}^* \Phi_a, \qquad H_2 \equiv \hat{w}_{\bar{a}}^* \Phi_a, \qquad (A7)$$

which can be inverted to yield $\Phi_a = H_1 \hat{v}_a + H_2 \hat{w}_a$. One can rewrite Eq. (A1) in terms of the Higgs basis fields,

$$\begin{aligned} -\mathcal{L}_{\mathrm{Y}} = {} & \overline{Q_L^0}(\tilde{H}_1 \kappa^{U,0} + \tilde{H}_2 \rho^{U,0}) U_R^0 \\ & + \bar{Q}_L^0 (H_1 \kappa^{D,0\dagger} + H_1 \rho^{D,0\dagger}) D_R^0 \\ & + \bar{E}_L^0 (H_1 \kappa^{E,0\dagger} + H_1 \rho^{E,0\dagger}) E_R^0 + \mathrm{H.c.}, \qquad (A8) \end{aligned}$$

The next step is to identify the quark and lepton mass-eigenstates. This is accomplished by replacing $H_1 \to (0, v/\sqrt{2})$ and performing unitary transformations of the left and right-handed up and down quark and lepton multiplets such that the resulting quark and charged lepton mass matrices are diagonal with non-negative entries. In more detail, we define:

$$\begin{aligned} P_L U &= V_L^U P_L U^0, & P_R U &= V_R^U P_R U^0, \\ P_L D &= V_L^D P_L D^0, & P_R D &= V_R^D P_R D^0, \\ P_L E &= V_L^E P_L E^0, & P_R E &= V_R^D P_R E^0, \\ P_L N &= V_L^E P_L N^0, & & (A9) \end{aligned}$$

and the Cabibbo-Kobayashi-Maskawa (CKM) matrix is defined as $K \equiv V_L^U V_L^{D\dagger}$. Note that for the neutrino fields, we are free to choose $V_L^N = V_L^E$ since neutrinos are exactly massless in this analysis. (Here we are ignoring the right-handed neutrino sector, which gives mass to neutrinos via the seesaw mechanism).

In particular, the unitary matrices V_L^F and V_R^F (for $F = U$, D and E) are chosen such that

$$M_U = \frac{v}{\sqrt{2}} V_L^U \kappa^{U,0} V_R^{U\dagger} = \mathrm{diag}(m_u, m_c, m_t), \quad (A10)$$

$$M_D = \frac{v}{\sqrt{2}} V_L^D \kappa^{D,0\dagger} V_R^{D\dagger} = \mathrm{diag}(m_d, m_s, m_b), \quad (A11)$$

$$M_E = \frac{v}{\sqrt{2}} V_L^E \kappa^{E,0\dagger} V_R^{E\dagger} = \mathrm{diag}(m_e, m_\mu, m_\tau). \quad (A12)$$

It is convenient to define

$$\kappa^U = V_L^U \kappa^{U,0} V_R^{U\dagger}, \qquad \kappa^D = V_R^D \kappa^{D,0} V_L^{D\dagger},$$
$$\kappa^E = V_R^D \kappa^{E,0} V_L^{E\dagger}, \quad (A13)$$
$$\rho^U = V_L^U \rho^{U,0} V_R^{U\dagger}, \qquad \rho^D = V_R^D \rho^{D,0} V_L^{D\dagger},$$
$$\rho^E = V_R^D \rho^{E,0} V_L^{E\dagger}. \quad (A14)$$

Equation (A6) implies that under the U(2) transformation, $\Phi_a \to U_{a\bar{b}} \Phi_b$,

$$\kappa^F \text{ is invariant and } \rho^F \to (\det U)\rho^F, \quad (A15)$$

for $F = U$, D and E. Indeed, κ^F is invariant since Eqs. (A10)–(A12) imply that

$$M_F = \frac{v}{\sqrt{2}} \kappa^F, \quad (A16)$$

which is a physical observable. The matrices ρ^U, ρ^D and ρ^E are independent pseudoinvariant complex 3×3 matrices. The Higgs-fermion interactions given in Eq. (A8) can be rewritten in terms of the quark and lepton mass eigenstates,

$$-\mathcal{L}_Y = \bar{U}_L(\kappa^U H_1^{0\dagger} + \rho^U H_2^{0\dagger})U_R - \bar{D}_L K^\dagger(\kappa^U H_1^- + \rho^U H_2^-)U_R + \bar{U}_L K(\kappa^{D\dagger} H_1^+ + \rho^{D\dagger} H_2^+)D_R + \bar{D}_L(\kappa^{D\dagger} H_1^0 + \rho^{D\dagger} H_2^0)D_R$$
$$+ \bar{N}_L(\kappa^{E\dagger} H_1^+ + \rho^{E\dagger} H_2^+)E_R + \bar{E}_L(\kappa^{E\dagger} H_1^0 + \rho^{E\dagger} H_2^0)E_R + \mathrm{H.c.} \quad (A17)$$

We now write down the renormalization group equations (RGEs) for the Yukawa matrices $\eta_a^{U,0}$, $\eta_a^{D,0}$ and $\eta_a^{E,0}$. Defining $\mathcal{D} \equiv 16\pi^2 \mu(d/d\mu)$, the RGEs are given by [43]

$$\mathcal{D}\eta_a^{U,0} = -\left(8g_s^2 + \frac{9}{4}g^2 + \frac{17}{12}g'^2\right)\eta_a^{U,0} + \{3\mathrm{Tr}[\eta_a^{U,0}(\eta_{\bar{b}}^{U,0})^\dagger$$
$$+ \eta_a^{D,0}(\eta_{\bar{b}}^{D,0})^\dagger] + \mathrm{Tr}[\eta_a^{E,0}(\eta_{\bar{b}}^{E,0})^\dagger]\}\eta_b^{U,0}$$
$$- 2(\eta_{\bar{b}}^{D,0})^\dagger \eta_a^{D,0} \eta_b^{U,0} + \eta_a^{U,0}(\eta_{\bar{b}}^{U,0})^\dagger \eta_b^{U,0}$$
$$+ \frac{1}{2}(\eta_{\bar{b}}^{D,0})^\dagger \eta_b^{D,0} \eta_a^{U,0} + \frac{1}{2}\eta_b^{U,0}(\eta_{\bar{b}}^{U,0})^\dagger \eta_a^{U,0}, \quad (A18)$$

$$\mathcal{D}\eta_a^{D,0} = -\left(8g_s^2 + \frac{9}{4}g^2 + \frac{5}{12}g'^2\right)\eta_a^{D,0} + \{3\mathrm{Tr}[(\eta_{\bar{b}}^{D,0})^\dagger \eta_a^{D,0}$$
$$+ (\eta_{\bar{b}}^{U,0})^\dagger \eta_a^{U,0}] + \mathrm{Tr}[(\eta_{\bar{b}}^{E,0})^\dagger \eta_a^{E,0}]\}\eta_b^{D,0}$$
$$- 2\eta_b^{D,0} \eta_a^{U,0}(\eta_{\bar{b}}^{U,0})^\dagger + \eta_b^{D,0}(\eta_{\bar{b}}^{D,0})^\dagger \eta_a^{D,0}$$
$$+ \frac{1}{2}\eta_a^{D,0} \eta_b^{U,0}(\eta_{\bar{b}}^{U,0})^\dagger + \frac{1}{2}\eta_a^{D,0}(\eta_{\bar{b}}^{D,0})^\dagger \eta_b^{D,0}, \quad (A19)$$

$$\mathcal{D}\eta_a^{E,0} = -\left(\frac{9}{4}g^2 + \frac{15}{4}g'^2\right)\eta_a^{E,0} + \{3\mathrm{Tr}[(\eta_{\bar{b}}^{D,0})^\dagger \eta_a^{D,0}$$
$$+ (\eta_{\bar{b}}^{U,0})^\dagger \eta_a^{U,0}] + \mathrm{Tr}[(\eta_{\bar{b}}^{E,0})^\dagger \eta_a^{E,0}]\}\eta_b^{E,0}$$
$$+ \eta_b^{E,0}(\eta_{\bar{b}}^{E,0})^\dagger \eta_a^{E,0} + \frac{1}{2}\eta_a^{E,0}(\eta_{\bar{b}}^{E,0})^\dagger \eta_b^{E,0}. \quad (A20)$$

The RGEs above are true for any basis choice. Thus, they must also be true in the Higgs basis in which $\hat{v} = (1, 0)$ and $\hat{w} = (0, 1)$. In this case, we can simply choose $\eta_1^{F,0} = \kappa^{F,0}$ and $\eta_2^{F,0} = \rho^{F,0}$ to obtain the RGEs for the $\kappa^{F,0}$ and $\rho^{F,0}$. Alternatively, we can multiply Eqs. (A18)–(A20) first by $\hat{v}_a^*$ and then by $\hat{w}_a^*$. Expanding $\eta_{\bar{a}}^\dagger$, which appears on the right-hand sides of Eqs. (A18)–(A20), in terms of $\kappa^\dagger$ and $\rho^\dagger$ using Eq. (A5), we again obtain the RGEs for the $\kappa^{F,0}$ and $\rho^{F,0}$. Of course, both methods must yield the same results, since the diagonalization matrices employed in Eqs. (A10)–(A12) are defined as those that bring the mass matrices to their diagonal form at the electroweak scale. No scale dependence is assumed in the diagonalization matrices, and as such they are not affected by the operators $\mathcal{D}$.

$$\mathcal{D}\kappa^{U,0} = -\left(8g_s^2 + \frac{9}{4}g^2 + \frac{17}{12}g'^2\right)\kappa^{U,0} + \{3\mathrm{Tr}[\kappa^{U,0}\kappa^{U,0\dagger} + \kappa^{D,0}\kappa^{D,0\dagger}] + \mathrm{Tr}[\kappa^{E,0}\kappa^{E,0\dagger}]\}\kappa^{U,0}$$
$$+ \{3\mathrm{Tr}[\kappa^{U,0}\rho^{U,0\dagger} + \kappa^{D,0}\rho^{D,0\dagger}] + \mathrm{Tr}[\kappa^{E,0}\rho^{E,0\dagger}]\}\rho^{U,0} - 2(\kappa^{D,0\dagger}\kappa^{D,0}\kappa^{U,0} + \rho^{D,0\dagger}\kappa^{D,0}\rho^{U,0})$$
$$+ \kappa^{U,0}(\kappa^{U,0\dagger}\kappa^{U,0} + \rho^{U,0\dagger}\rho^{U,0}) + \frac{1}{2}(\kappa^{D,0\dagger}\kappa^{D,0} + \rho^{D,0\dagger}\rho^{D,0})\kappa^{U,0} + \frac{1}{2}(\kappa^{U,0}\kappa^{U,0\dagger} + \rho^{U,0}\rho^{U,0\dagger})\kappa^{U,0},$$

$$
\begin{aligned}
\mathcal{D}\rho^{U,0} =& -\left(8g_s^2 + \frac{9}{4}g^2 + \frac{17}{12}g'^2\right)\rho^{U,0} + \{3\mathrm{Tr}[\rho^{U,0}\kappa^{U,0\dagger} + \rho^{D,0}\kappa^{D,0\dagger}] + \mathrm{Tr}[\rho^{E,0}\kappa^{E,0\dagger}]\}\kappa^{U,0} \\
&+ \{3\mathrm{Tr}[\rho^{U,0}\rho^{U,0\dagger} + \rho^{D,0}\rho^{D,0\dagger}] + \mathrm{Tr}[\rho^{E,0}\rho^{E,0\dagger}]\}\rho^{U,0} - 2(\kappa^{D,0\dagger}\rho^{D,0}\kappa^{U,0} + \rho^{D,0\dagger}\rho^{D,0}\rho^{U,0}) \\
&+ \rho^{U,0}(\kappa^{U,0\dagger}\kappa^{U,0} + \rho^{U,0\dagger}\rho^{U,0}) + \frac{1}{2}(\kappa^{D,0\dagger}\kappa^{D,0} + \rho^{D,0\dagger}\rho^{D,0})\rho^{U,0} + \frac{1}{2}(\kappa^{U,0}\kappa^{U,0\dagger} + \rho^{U,0}\rho^{U,0\dagger})\rho^{U,0},
\end{aligned}
$$

$$
\begin{aligned}
\mathcal{D}\kappa^{D,0} =& -\left(8g_s^2 + \frac{9}{4}g^2 + \frac{5}{12}g'^2\right)\kappa^{D,0} + \{3\mathrm{Tr}[\kappa^{D,0\dagger}\kappa^{D,0} + \kappa^{U,0\dagger}\kappa^{U,0}] + \mathrm{Tr}[\kappa^{E,0\dagger}\kappa^{E,0}]\}\kappa^{D,0} \\
&+ \{3\mathrm{Tr}[\rho^{D,0\dagger}\kappa^{D,0} + \rho^{U,0\dagger}\kappa^{U,0}] + \mathrm{Tr}[\rho^{E,0\dagger}\kappa^{E,0}]\}\rho^{D,0} - 2(\kappa^{D,0}\kappa^{U,0}\kappa^{U,0\dagger} + \rho^{D,0}\kappa^{U,0}\rho^{U,0\dagger}) \\
&+ (\kappa^{D,0}\kappa^{D,0\dagger} + \rho^{D,0}\rho^{D,0\dagger})\kappa^{D,0} + \frac{1}{2}\kappa^{D,0}(\kappa^{U,0}\kappa^{U,0\dagger} + \rho^{U,0}\rho^{U,0\dagger}) + \frac{1}{2}\kappa^{D,0}(\kappa^{D,0\dagger}\kappa^{D,0} + \rho^{D,0\dagger}\rho^{D,0}),
\end{aligned}
$$

$$
\begin{aligned}
\mathcal{D}\rho^{D,0} =& -\left(8g_s^2 + \frac{9}{4}g^2 + \frac{5}{12}g'^2\right)\rho^{D,0} + \{3\mathrm{Tr}[\kappa^{D,0\dagger}\rho^{D,0} + \kappa^{U,0\dagger}\rho^{U,0}] + \mathrm{Tr}[\kappa^{E,0\dagger}\rho^{E,0}]\}\kappa^{D,0} \\
&+ \{3\mathrm{Tr}[\rho^{D,0\dagger}\rho^{D,0} + \rho^{U,0\dagger}\rho^{U,0}] + \mathrm{Tr}[\rho^{E,0\dagger}\rho^{E,0}]\}\rho^{D,0} - 2(\kappa^{D,0}\rho^{U,0}\kappa^{U,0\dagger} + \rho^{D,0}\rho^{U,0}\rho^{U,0\dagger}) \\
&+ (\kappa^{D,0}\kappa^{D,0\dagger} + \rho^{D,0}\rho^{D,0\dagger})\rho^{D,0} + \frac{1}{2}\rho^{D,0}(\kappa^{U,0}\kappa^{U,0\dagger} + \rho^{U,0}\rho^{U,0\dagger}) + \frac{1}{2}\rho^{D,0}(\kappa^{D,0\dagger}\kappa^{D,0} + \rho^{D,0\dagger}\rho^{D,0}),
\end{aligned}
$$

$$
\begin{aligned}
\mathcal{D}\kappa^{E,0} =& -\left(\frac{9}{4}g^2 + \frac{15}{4}g'^2\right)\kappa^{E,0} + \{3\mathrm{Tr}[\kappa^{D,0\dagger}\kappa^{D,0} + \kappa^{U,0\dagger}\kappa^{U,0}] + \mathrm{Tr}[\kappa^{E,0\dagger}\kappa^{E,0}]\}\kappa^{E,0} + \{3\mathrm{Tr}[\rho^{D,0\dagger}\kappa^{D,0} + \rho^{U,0\dagger}\kappa^{U,0}] \\
&+ \mathrm{Tr}[\rho^{E,0\dagger}\kappa^{E,0}]\}\rho^{E,0} + (\kappa^{E,0}\kappa^{E,0\dagger} + \rho^{E,0}\rho^{E,0\dagger})\kappa^{E,0} + \frac{1}{2}\kappa^{E,0}(\kappa^{E,0\dagger}\kappa^{E,0} + \rho^{E,0\dagger}\rho^{E,0}),
\end{aligned}
$$

$$
\begin{aligned}
\mathcal{D}\rho^{E,0} =& -\left(\frac{9}{4}g^2 + \frac{15}{4}g'^2\right)\rho^{E,0} + \{3\mathrm{Tr}[\kappa^{D,0\dagger}\rho^{D,0} + \kappa^{U,0\dagger}\rho^{U,0}] + \mathrm{Tr}[\kappa^{E,0\dagger}\rho^{E,0}]\}\kappa^{E,0} + \{3\mathrm{Tr}[\rho^{D,0\dagger}\rho^{D,0} + \rho^{U,0\dagger}\rho^{U,0}] \\
&+ \mathrm{Tr}[\rho^{E,0\dagger}\rho^{E,0}]\}\rho^{E,0} + (\kappa^{E}\kappa^{E,0\dagger} + \rho^{E,0}\rho^{E,0\dagger})\rho^{E,0} + \frac{1}{2}\rho^{E,0}(\kappa^{E,0\dagger}\kappa^{E,0} + \rho^{E,0\dagger}\rho^{E,0}).
\end{aligned}
$$

Using Eqs. (A13) and (A14), we immediately obtain the RGEs for the κ^F and ρ^F,

$$
\begin{aligned}
\mathcal{D}\kappa^{U} =& -\left(8g_s^2 + \frac{9}{4}g^2 + \frac{17}{12}g'^2\right)\kappa^{U} + \{3\mathrm{Tr}[\kappa^{U}\kappa^{U\dagger} + \kappa^{D}\kappa^{D\dagger}] + \mathrm{Tr}[\kappa^{E}\kappa^{E\dagger}]\}\kappa^{U} \\
&+ \{3\mathrm{Tr}[\kappa^{U}\rho^{U\dagger} + \kappa^{D}\rho^{D\dagger}] + \mathrm{Tr}[\kappa^{E}\rho^{E\dagger}]\}\rho^{U} - 2K(\kappa^{D\dagger}\kappa^{D}K^{\dagger}\kappa^{U} + \rho^{D\dagger}\kappa^{D}K^{\dagger}\rho^{U}) \\
&+ \kappa^{U}(\kappa^{U\dagger}\kappa^{U} + \rho^{U\dagger}\rho^{U}) + \frac{1}{2}K(\kappa^{D\dagger}\kappa^{D} + \rho^{D\dagger}\rho^{D})K^{\dagger}\kappa^{U} + \frac{1}{2}(\kappa^{U}\kappa^{U\dagger} + \rho^{U}\rho^{U\dagger})\kappa^{U}, \quad\quad\text{(A21)}
\end{aligned}
$$

$$
\begin{aligned}
\mathcal{D}\rho^{U} =& -\left(8g_s^2 + \frac{9}{4}g^2 + \frac{17}{12}g'^2\right)\rho^{U} + \{3\mathrm{Tr}[\rho^{U}\kappa^{U\dagger} + \rho^{D}\kappa^{D\dagger}] + \mathrm{Tr}[\rho^{E}\kappa^{E\dagger}]\}\kappa^{U} \\
&+ \{3\mathrm{Tr}[\rho^{U}\rho^{U\dagger} + \rho^{D}\rho^{D\dagger}] + \mathrm{Tr}[\rho^{E}\rho^{E\dagger}]\}\rho^{U} - 2K(\kappa^{D\dagger}\rho^{D}K^{\dagger}\kappa^{U} + \rho^{D\dagger}\rho^{D}K^{\dagger}\rho^{U}) \\
&+ \rho^{U}(\kappa^{U\dagger}\kappa^{U} + \rho^{U\dagger}\rho^{U}) + \frac{1}{2}K(\kappa^{D\dagger}\kappa^{D} + \rho^{D\dagger}\rho^{D})K^{\dagger}\rho^{U} + \frac{1}{2}(\kappa^{U}\kappa^{U\dagger} + \rho^{U}\rho^{U\dagger})\rho^{U}, \quad\quad\text{(A22)}
\end{aligned}
$$

$$
\begin{aligned}
\mathcal{D}\kappa^{D} =& -\left(8g_s^2 + \frac{9}{4}g^2 + \frac{5}{12}g'^2\right)\kappa^{D} + \{3\mathrm{Tr}[\kappa^{D\dagger}\kappa^{D} + \kappa^{U\dagger}\kappa^{U}] + \mathrm{Tr}[\kappa^{E\dagger}\kappa^{E}]\}\kappa^{D} \\
&+ \{3\mathrm{Tr}[\rho^{D\dagger}\kappa^{D} + \rho^{U\dagger}\kappa^{U}] + \mathrm{Tr}[\rho^{E\dagger}\kappa^{E}]\}\rho^{D} - 2(\kappa^{D}K^{\dagger}\kappa^{U}\kappa^{U\dagger} + \rho^{D}K^{\dagger}\kappa^{U}\rho^{U\dagger})K \\
&+ (\kappa^{D}\kappa^{D\dagger} + \rho^{D}\rho^{D\dagger})\kappa^{D} + \frac{1}{2}\kappa^{D}K^{\dagger}(\kappa^{U}\kappa^{U\dagger} + \rho^{U}\rho^{U\dagger})K + \frac{1}{2}\kappa^{D}(\kappa^{D\dagger}\kappa^{D} + \rho^{D\dagger}\rho^{D}), \quad\quad\text{(A23)}
\end{aligned}
$$

$$
\begin{aligned}
\mathcal{D}\rho^{D} =& -\left(8g_s^2 + \frac{9}{4}g^2 + \frac{5}{12}g'^2\right)\rho^{D} + \{3\mathrm{Tr}[\kappa^{D\dagger}\rho^{D} + \kappa^{U\dagger}\rho^{U}] + \mathrm{Tr}[\kappa^{E\dagger}\rho^{E}]\}\kappa^{D} \\
&+ \{3\mathrm{Tr}[\rho^{D\dagger}\rho^{D} + \rho^{U\dagger}\rho^{U}] + \mathrm{Tr}[\rho^{E\dagger}\rho^{E}]\}\rho^{D} - 2(\kappa^{D}K^{\dagger}\rho^{U}\kappa^{U\dagger} + \rho^{D}K^{\dagger}\rho^{U}\rho^{U\dagger})K \\
&+ (\kappa^{D}\kappa^{D\dagger} + \rho^{D}\rho^{D\dagger})\rho^{D} + \frac{1}{2}\rho^{D}K^{\dagger}(\kappa^{U}\kappa^{U\dagger} + \rho^{U}\rho^{U\dagger})K + \frac{1}{2}\rho^{D}(\kappa^{D\dagger}\kappa^{D} + \rho^{D\dagger}\rho^{D}), \quad\quad\text{(A24)}
\end{aligned}
$$

$$\mathcal{D}\kappa^E = -\left(\frac{9}{4}g^2 + \frac{15}{4}g'^2\right)\kappa^E + \{3\text{Tr}[\kappa^{D\dagger}\kappa^D + \kappa^{U\dagger}\kappa^U] + \text{Tr}[\kappa^{E\dagger}\kappa^E]\}\kappa^E + \{3\text{Tr}[\rho^{D\dagger}\kappa^D + \rho^{U\dagger}\kappa^U] + \text{Tr}[\rho^{E\dagger}\kappa^E]\}\rho^E$$

$$+ (\kappa^E\kappa^{E\dagger} + \rho^E\rho^{E\dagger})\kappa^E + \frac{1}{2}\kappa^E(\kappa^{E\dagger}\kappa^E + \rho^{E\dagger}\rho^E), \tag{A25}$$

$$\mathcal{D}\rho^E = -\left(\frac{9}{4}g^2 + \frac{15}{4}g'^2\right)\rho^E + \{3\text{Tr}[\kappa^{D\dagger}\rho^D + \kappa^{U\dagger}\rho^U] + \text{Tr}[\kappa^{E\dagger}\rho^E]\}\kappa^E + \{3\text{Tr}[\rho^{D\dagger}\rho^D + \rho^{U\dagger}\rho^U] + \text{Tr}[\rho^{E\dagger}\rho^E]\}\rho^E$$

$$+ (\kappa^E\kappa^{E\dagger} + \rho^E\rho^{E\dagger})\rho^E + \frac{1}{2}\rho^E(\kappa^{E\dagger}\kappa^E + \rho^{E\dagger}\rho^E). \tag{A26}$$

The 2HDM scalar potential in a generic basis shown in Eq. (1) can be written in a more compact form following the notation of Ref. [39],

$$\mathcal{V} = Y_{a\bar{b}}(\Phi_{\bar{a}}^\dagger\Phi_b) + \frac{1}{2}Z_{a\bar{b}c\bar{d}}(\Phi_{\bar{a}}^\dagger\Phi_b)(\Phi_{\bar{c}}^\dagger\Phi_d). \tag{A27}$$

Hermiticity requires that $Y_{a\bar{b}} = Y_{b\bar{a}}^*$ and $Z_{a\bar{b}c\bar{d}} = Z_{d\bar{c}b\bar{a}}^*$. In addition, the form of the scalar potential given in Eq. (A27) implies that $Z_{a\bar{b}c\bar{d}} = Z_{c\bar{d}a\bar{b}}$. The full one-loop β function for $Z_{a\bar{b}c\bar{d}}$ is given by

$$\mathcal{D}Z_{a\bar{b}c\bar{d}} = 4Z_{a\bar{b}e\bar{f}}Z_{c\bar{d}f\bar{e}} + 2Z_{a\bar{f}e\bar{d}}Z_{c\bar{d}f\bar{e}} + 2Z_{a\bar{f}c\bar{e}}Z_{f\bar{b}e\bar{d}} + 2Z_{a\bar{b}e\bar{f}}Z_{c\bar{e}f\bar{d}} + 2Z_{a\bar{e}f\bar{b}}Z_{c\bar{d}e\bar{f}} - (3g'^2 + 9g^2)Z_{a\bar{b}c\bar{d}}$$

$$+ \frac{3}{4}(3g^4 - 2g'^2g^2 + g'^4)\delta_{a\bar{b}}\delta_{c\bar{d}} + (3g'^2g^2)\delta_{a\bar{d}}\delta_{c\bar{b}} - 4N_c\text{Tr}[\eta_a^Q\eta_{\bar{b}}^{Q\dagger}\eta_c^Q\eta_{\bar{d}}^{Q\dagger}]$$

$$+ 4(\text{Tr}[\eta_{\bar{e}}^{Q\dagger}\eta_a^Q]Z_{e\bar{b}c\bar{d}} + \text{Tr}[\eta_{\bar{b}}^{Q\dagger}\eta_e^Q]Z_{a\bar{e}c\bar{d}} + \text{Tr}[\eta_{\bar{e}}^{Q\dagger}\eta_c^Q]Z_{a\bar{b}e\bar{d}} + \text{Tr}[\eta_{\bar{d}}^{Q\dagger}\eta_e^Q]Z_{a\bar{b}c\bar{e}}). \tag{A28}$$

The squared-mass and coupling coefficients of the 2HDM scalar potential in the Higgs basis [cf. Eq. (3)] can be written in the form of invariants or pseudoinvariants with respect to the U(2) transformations, $\Phi_a \to U_{a\bar{b}}\Phi_b$, as shown in Ref. [39]. The three squared-mass parameters are given by

$$Y_1 \equiv Y_{a\bar{b}}\hat{v}_{\bar{a}}^*\hat{v}_b, \qquad Y_2 \equiv Y_{a\bar{b}}\hat{w}_{\bar{a}}^*\hat{w}_b, \qquad Y_3 \equiv Y_{a\bar{b}}\hat{v}_{\bar{a}}^*\hat{w}_b, \tag{A29}$$

and seven coupling parameters are given by

$$Z_1 \equiv Z_{a\bar{b}c\bar{d}}\hat{v}_{\bar{a}}^*\hat{v}_b\hat{v}_{\bar{c}}^*\hat{v}_d, \qquad Z_2 \equiv Z_{a\bar{b}c\bar{d}}\hat{w}_{\bar{a}}^*\hat{w}_b\hat{w}_{\bar{c}}^*\hat{w}_d, \tag{A30}$$

$$Z_3 \equiv Z_{a\bar{b}c\bar{d}}\hat{v}_{\bar{a}}^*\hat{v}_b\hat{w}_{\bar{c}}^*\hat{w}_d, \qquad Z_4 \equiv Z_{a\bar{b}c\bar{d}}\hat{w}_{\bar{a}}^*\hat{v}_b\hat{v}_{\bar{c}}^*\hat{w}_d, \tag{A31}$$

$$Z_5 \equiv Z_{a\bar{b}c\bar{d}}\hat{v}_{\bar{a}}^*\hat{w}_b\hat{v}_{\bar{c}}^*\hat{w}_d, \tag{A32}$$

$$Z_6 \equiv Z_{a\bar{b}c\bar{d}}\hat{v}_{\bar{a}}^*\hat{v}_b\hat{v}_{\bar{c}}^*\hat{w}_d, \tag{A33}$$

$$Z_7 \equiv Z_{a\bar{b}c\bar{d}}\hat{v}_{\bar{a}}^*\hat{w}_b\hat{w}_{\bar{c}}^*\hat{w}_d. \tag{A34}$$

Note that under a U(2) transformation, $\hat{v}_a \to U_{a\bar{b}}\hat{v}_b$, whereas

$$\hat{w}_a \to (\det U)^{-1}U_{a\bar{b}}\hat{w}_b. \tag{A35}$$

Consequently, Y_1, Y_2, $Z_{1,2,3,4}$ are real U(2) invariants, whereas Y_3, $Z_{5,6,7}$ are potentially complex U(2) pseudoinvariants, which are rephased under a U(2) transformation,

$$[Y_3, Z_6, Z_7] \to (\det U)^{-1}[Y_3, Z_6, Z_7] \quad \text{and} \quad Z_5 \to (\det U)^{-2}Z_5. \tag{A36}$$

Using the above results in Eq. (A28), the one-loop RGEs for the quartic scalar couplings in the Higgs basis are as follows:

$$
\mathcal{D}Z_1 = 12Z_1^2 + 4Z_3^2 + 4Z_3Z_4 + 2Z_4^2 + 2|Z_5|^2 + 24|Z_6|^2 - (3g'^2 + 9g^2)Z_1 + \frac{3}{4}(g'^4 + 2g'^2g^2 + 3g^4)
$$
$$
- 4N_c\mathrm{Tr}[\kappa^{Q\dagger}\kappa^Q\kappa^{Q\dagger}\kappa^Q] + 16(2\mathrm{Tr}[\kappa^{Q\dagger}\kappa^Q]Z_1 + \mathrm{Tr}[\kappa^{Q\dagger}\rho^Q]Z_6 + \mathrm{Tr}[\rho^{Q\dagger}\kappa^Q]Z_6^*), \tag{A37}
$$

$$
\mathcal{D}Z_2 = 12Z_2^2 + 4Z_3^2 + 4Z_3Z_4 + 2Z_4^2 + 2|Z_5|^2 + 24|Z_7|^2 - (3g'^2 + 9g^2)Z_2 + \frac{3}{4}(g'^4 + 2g'^2g^2 + 3g^4)
$$
$$
- 4N_c\mathrm{Tr}[\rho^{Q\dagger}\rho^Q\rho^{Q\dagger}\rho^Q] + 8(2\mathrm{Tr}[\rho^{Q\dagger}\rho^Q]Z_2 + \mathrm{Tr}[\kappa^{Q\dagger}\rho^Q]Z_7 + \mathrm{Tr}[\rho^{Q\dagger}\kappa^Q]Z_7^*), \tag{A38}
$$

$$
\mathcal{D}Z_3 = 2(Z_1 + Z_2)(3Z_3 + Z_4) + 4Z_3^2 + 2Z_4^2 + 2|Z_5|^2 + 4|Z_6|^2 + 4|Z_7|^2 + 8Z_6Z_7^* + 8Z_6^*Z_7
$$
$$
- (3g'^2 + 9g^2)Z_3 + \frac{3}{4}(g'^4 - 2g'^2g^2 + 3g^4) - 4N_c\mathrm{Tr}[\kappa^{Q\dagger}\kappa^Q\rho^{Q\dagger}\rho^Q] + 4(2\mathrm{Tr}[\kappa^{Q\dagger}\kappa^Q]Z_3
$$
$$
+ 2\mathrm{Tr}[\rho^{Q\dagger}\rho^Q]Z_3 + \mathrm{Tr}[\kappa^{Q\dagger}\rho^Q]Z_6 + \mathrm{Tr}[\rho^{Q\dagger}\kappa^Q]Z_6^* + \mathrm{Tr}[\kappa^{Q\dagger}\rho^Q]Z_7 + \mathrm{Tr}[\rho^{Q\dagger}\kappa^Q]Z_7^*), \tag{A39}
$$

$$
\mathcal{D}Z_4 = 2(Z_1 + Z_2)Z_4 + 8Z_3Z_4 + 4Z_4^2 + 8|Z_5|^2 + 10|Z_6|^2 + 10|Z_7|^2 + 2Z_6Z_7^* + 2Z_6^*Z_7
$$
$$
- (3g'^2 + 9g^2)Z_4 + \frac{3}{2}g'^2g^2 - 4N_c\mathrm{Tr}[\kappa^{Q\dagger}\rho^Q\rho^{Q\dagger}\kappa^Q] + 4(2\mathrm{Tr}[\kappa^{Q\dagger}\kappa^Q]Z_4 + 2\mathrm{Tr}[\rho^{Q\dagger}\rho^Q]Z_4
$$
$$
+ \mathrm{Tr}[\kappa^{Q\dagger}\rho^Q]Z_6 + \mathrm{Tr}[\rho^{Q\dagger}\kappa^Q]Z_6^* + \mathrm{Tr}[\kappa^{Q\dagger}\rho^Q]Z_7 + \mathrm{Tr}[\rho^{Q\dagger}\kappa^Q]Z_7^*), \tag{A40}
$$

$$
\mathcal{D}Z_5 = 2Z_5(Z_1 + Z_2 + 4Z_3 + 6Z_4) + 10Z_6^2 + 10Z_7^2 + 4Z_6Z_7 - (3g'^2 + 9g^2)Z_5 - 4N_c\mathrm{Tr}[\kappa^{Q\dagger}\rho^Q\kappa^{Q\dagger}\rho^Q]
$$
$$
+ 8(\mathrm{Tr}[\kappa^{Q\dagger}\kappa^Q]Z_5 + \mathrm{Tr}[\rho^{Q\dagger}\rho^Q]Z_5 + \mathrm{Tr}[\rho^{Q\dagger}\kappa^Q]Z_6 + \mathrm{Tr}[\rho^{Q\dagger}\kappa^Q]Z_7), \tag{A41}
$$

$$
\mathcal{D}Z_6 = 12Z_1Z_6 + 6Z_3(Z_6 + Z_7) + 4Z_4(2Z_6 + Z_7) + 2Z_5(5Z_6^* + Z_7^*) - (3g'^2 + 9g^2)Z_6
$$
$$
- 4N_c\mathrm{Tr}[\kappa^{Q\dagger}\kappa^Q\kappa^{Q\dagger}\rho^Q] + 4(3\mathrm{Tr}[\kappa^{Q\dagger}\kappa^Q]Z_6 + \mathrm{Tr}[\rho^{Q\dagger}\rho^Q]Z_6 + \mathrm{Tr}[\rho^{Q\dagger}\kappa^Q]Z_1
$$
$$
+ \mathrm{Tr}[\rho^{Q\dagger}\kappa^Q]Z_3 + \mathrm{Tr}[\rho^{Q\dagger}\kappa^Q]Z_4 + \mathrm{Tr}[\kappa^{Q\dagger}\rho^Q]Z_5), \tag{A42}
$$

$$
\mathcal{D}Z_7 = 12Z_2Z_7 + 6Z_3(Z_6 + Z_7) + 4Z_4(Z_6 + 2Z_7) + 2Z_5(Z_6^* + 5Z_7^*) - (3g'^2 + 9g^2)Z_7
$$
$$
- 4N_c\mathrm{Tr}[\rho^{Q\dagger}\rho^Q\rho^{Q\dagger}\rho^Q] + 4(3\mathrm{Tr}[\rho^{Q\dagger}\rho^Q]Z_7 + \mathrm{Tr}[\kappa^{Q\dagger}\kappa^Q]Z_7 + \mathrm{Tr}[\rho^{Q\dagger}\kappa^Q]Z_2 + \mathrm{Tr}[\rho^{Q\dagger}\kappa^Q]Z_3
$$
$$
+ \mathrm{Tr}[\rho^{Q\dagger}\kappa^Q]Z_4 + \mathrm{Tr}[\kappa^{Q\dagger}\rho^Q]Z_5). \tag{A43}
$$

Finally, we note that the anomalous dimensions, which contribute to the quartic scalar coupling β functions, are given by

$$
\gamma_{a\bar{b}} = -\frac{1}{32\pi^2}(3g'^2 + 9g^2)\delta_{a\bar{b}} + \frac{1}{4\pi^2}\mathrm{Tr}[\eta_a^Q\eta_{\bar{b}}^{Q\dagger}]. \tag{A44}
$$

APPENDIX B: BOUNDED FROM BELOW CONDITIONS FOR A GENERAL 2HDM POTENTIAL

To ensure the existence of a stable vacuum, the 2HDM scalar potential must be bounded from below; i.e., it must assume positive values for any direction for which the fields are tending to infinity. This places some restrictions on the allowed values of the quartic scalar couplings. For the case of the scalar potential given in Eq. (1) with

$\lambda_6 = \lambda_7 = 0$, those necessary and sufficient conditions are given in Eqs. (23)–(26).

We now review the analogous conditions for the most general renormalizable 2HDM potential, found in Refs. [54,62]. It is particularly convenient to introduce a new notation for the scalar potential, based on gauge invariant field bilinears. Indeed, in many 2HDM studies, such as the comparison of the value of the potential in different vacua, the classification of scalar symmetries and stability conditions, the bilinear formalism provides a significant simplification in the calculations. This formalism also reveals a hidden Minkowski structure in the potential, which was established in Refs. [54,62]. A similar Minkowskian notation has been employed in Refs. [63,64].

There are four independent gauge-invariant field bilinears, which are defined by

$$r_0 = \Phi_1^\dagger \Phi_1 + \Phi_2^\dagger \Phi_2,$$

$$r_1 = -(\Phi_1^\dagger \Phi_2 + \Phi_2^\dagger \Phi_1) = -2\mathrm{Re}(\Phi_1^\dagger \Phi_2),$$

$$r_2 = i(\Phi_1^\dagger \Phi_2 - \Phi_2^\dagger \Phi_1) = -2\mathrm{Im}(\Phi_1^\dagger \Phi_2),$$

$$r_3 = -(\Phi_1^\dagger \Phi_1 - \Phi_2^\dagger \Phi_2). \tag{B1}$$

These four quantities form the components of a covariant four-vector, $r_\mu = (r_0, \vec{r})$ with respect to SO(3,1) transformations. We also define $r^\mu = g^{\mu\nu} r_\nu = (r_0, -\vec{r})$ where $g^{\mu\nu}$ is the usual Minkowski metric. It is straightforward to verify that $r_0 \geq 0$ and $r^\mu r_\mu \geq 0$, the latter being a consequence of the Schwarz inequality. That is, the four-vector r_μ lives on or inside the forward lightcone LC^+. The vacuum that preserves $\mathrm{SU}(2) \times \mathrm{U}(1)$ electroweak symmetry [i.e., $\langle \Phi_1 \rangle = \langle \Phi_2 \rangle = 0$] corresponds to the apex of LC^+; all neutral vacua correspond to the surface of LC^+, and any charge breaking vacua would lie on the interior of

LC^+. Transformations of the scalar fields that preserve the scalar field kinetic energy terms leave r_0 invariant and correspond to SO(3) rotations of the three-vectors, $\vec{r}$.

In terms of the bilinears defined in Eq. (B1), the scalar potential of Eq. (3) can be written as

$$\mathcal{V} = -M_\mu r^\mu + \frac{1}{2} r^\mu \Lambda_\mu{}^\nu r_\nu, \tag{B2}$$

with the 4-vector M_μ and the mixed tensor $\Lambda_\mu{}^\nu$ given by

$$M_\mu = \left(-\frac{1}{2}(Y_1 + Y_2), \ \mathrm{Re}Y_3, \ -\mathrm{Im}Y_3, \ -\frac{1}{2}(Y_1 - Y_2) \right) \tag{B3}$$

and

$$\Lambda_\mu{}^\nu = \frac{1}{2} \begin{pmatrix} \frac{1}{2}(Z_1 + Z_2) + Z_3 & -\mathrm{Re}(Z_6 + Z_7) & \mathrm{Im}(Z_6 + Z_7) & -\frac{1}{2}(Z_1 - Z_2) \\ \mathrm{Re}(Z_6 + Z_7) & -Z_4 - \mathrm{Re}Z_5 & \mathrm{Im}Z_5 & -\mathrm{Re}(Z_6 - Z_7) \\ -\mathrm{Im}(Z_6 + Z_7) & \mathrm{Im}Z_5 & -Z_4 + \mathrm{Re}Z_5 & \mathrm{Im}(Z_6 - Z_7) \\ \frac{1}{2}(Z_1 - Z_2) & -\mathrm{Re}(Z_6 - Z_7) & \mathrm{Im}(Z_6 - Z_7) & -\frac{1}{2}(Z_1 + Z_2) + Z_3 \end{pmatrix}. \tag{B4}$$

To ensure that the scalar potential is bounded from below one needs to evaluate the eigenvalues and eigenvectors of the matrix $\Lambda_\mu{}^\nu$. Then one can determine conditions on those eigenvalues and eigenvectors such that $r^\mu \Lambda_\mu{}^\nu r_\nu \geq 0$. The eigenvalues Λ_a ($a = 0, 1, 2, 3$) of the matrix $\Lambda_\mu{}^\nu$ will be determined by the usual characteristic equation,

$$\det(\Lambda_\mu{}^\nu - \Lambda_a g_\mu{}^\nu) = 0. \tag{B5}$$

since $g_\mu{}^\nu = \delta_\mu^\nu$ is just the 4×4 identity matrix. The corresponding eigenvectors corresponding to eigenvalue Λ_a will be denoted by $V^{(a)}$. For the most general 2HDM potential, the eigenvalues are the solutions of a quartic equation, which can in principle be determined analytically (although the corresponding expressions are not particularly transparent). However, it is straightforward to numerically evaluate the eigenvalues and corresponding eigenvectors. Note that, in general, some of the eigenvalues may be complex (since the real matrix $\Lambda_\mu{}^\nu$ is not symmetric unless $Z_6 = Z_7 = 0$ and $Z_1 = Z_2$).

Having evaluated the eigenvalues and eigenvectors of $\Lambda_\mu{}^\nu$, we make use of *Proposition 10* of Ref. [54] to conclude that the 2HDM potential is bounded from below *if and only if* the following conditions are met:

(1) All the eigenvalues Λ_a are real.

(2) $\Lambda_0 > 0$.

(3) $\Lambda_0 > \{\Lambda_1, \Lambda_2, \Lambda_3\}$. There may or may not be degeneracies among the three eigenvalues Λ_i ($i = 1, 2, 3$).

(4) There exist four linearly independent eigenvectors $V^{(a)}$ corresponding to the four eigenvalues Λ_a, for $a = 0, 1, 2, 3$.

(5) The eigenvector $V^{(0)} = (v_{00}, v_{10}, v_{20}, v_{30})$, corresponding to the eigenvalue Λ_0, is real and timelike. That is, it can be normalized so that

$$|V^{(0)}|^2 = v_{00}^2 - v_{10}^2 - v_{20}^2 - v_{30}^2 = 1.$$

(6) The remaining three eigenvectors $V^{(i)} = (v_{0i}, v_{1i}, v_{2i}, v_{3i})$ are real and spacelike, i.e. normalized so that

$$|V^{(i)}|^2 = v_{0i}^2 - v_{1i}^2 - v_{2i}^2 - v_{3i}^2 = -1.$$

To illustrate this technique, we shall reproduce the bounded from below conditions for a potential with a $\mathbb{Z}_2$ symmetry in the Higgs basis so that $Z_6 = Z_7 = 0$. Without loss of generality, we can choose Z_5 real by rephasing the Higgs basis field H_2. The matrix $\Lambda = \Lambda_\mu{}^\nu$ is then given by

$$\Lambda = \frac{1}{2} \begin{pmatrix} \frac{1}{2}(Z_1 + Z_2) + Z_3 & 0 & 0 & -\frac{1}{2}(Z_1 - Z_2) \\ 0 & -Z_4 - Z_5 & 0 & 0 \\ 0 & 0 & -Z_4 + Z_5 & 0 \\ \frac{1}{2}(Z_1 - Z_2) & 0 & 0 & -\frac{1}{2}(Z_1 + Z_2) + Z_3 \end{pmatrix}, \quad (B6)$$

so that two of its eigenvalues can be immediately read off as $\Lambda_1 = -Z_4 - Z_5$ and $\Lambda_2 = -Z_4 + Z_5$. The remaining two eigenvalues are

$$\Lambda_{\pm} = Z_3 \pm \sqrt{Z_1 Z_2}. \quad (B7)$$

Since the eigenvalues must be real, if follows that

$$Z_1 Z_2 > 0. \quad (B8)$$

Λ_+ is the largest eigenvalue and thus must corresponds to the timelike eigenvector. Hence, we identify $\Lambda_0 = Z_3 + \sqrt{Z_1 Z_2}$ and $\Lambda_3 = Z_3 - \sqrt{Z_1 Z_2}$. Imposing the requirement that the scalar potential is bounded from below, it follows that the eigenvalues obtained above must all be real and obey the following inequalities:

$$\Lambda_0 > 0 \Rightarrow Z_3 > -\sqrt{Z_1 Z_2} \quad (B9)$$

$$\Lambda_0 > \{\Lambda_1, \Lambda_2, \Lambda_3\} \Rightarrow Z_3 + Z_4 - |Z_5| > -\sqrt{Z_1 Z_2}, \quad (B10)$$

which are the Higgs basis equivalents of Eqs. (25) and (26). The timelike eigenvector is $V^{(0)} = (x, 0, 0, y)$, where the components x and y are related via the eigenvector equation by

$$y = \frac{Z_1 + Z_2 - \sqrt{Z_1 Z_2}}{Z_1 - Z_2} x. \quad (B11)$$

Since the timelike normalization condition implies that $x^2 - y^2 = 1$, we obtain

$$x^2 = \frac{(Z_1 - Z_2)^2}{4\sqrt{Z_1 Z_2}(Z_1 + Z_2)}. \quad (B12)$$

Thus we see that we must have $Z_1 + Z_2 > 0$, which when combined with Eq. (B8) yields

$$Z_1 > 0, \qquad Z_2 > 0. \quad (B13)$$

Thus we recover the Higgs basis equivalents of Eqs. (23) and (24).

[1] G. Aad *et al.* (ATLAS Collaboration), Phys. Lett. B **716**, 1 (2012).
[2] S. Chatrchyan *et al.* (CMS Collaboration), Phys. Lett. B **716**, 30 (2012).
[3] L. Maiani, A. D. Polosa, and V. Riquer, Phys. Lett. B **724**, 274 (2013).
[4] A. Arbey, M. Battaglia, and F. Mahmoudi, Phys. Rev. D **88**, 015007 (2013).
[5] N. Cabibbo, L. Maiani, G. Parisi, and R. Petronzio, Nucl. Phys. **B158**, 295 (1979).
[6] M. Lindner, Z. Phys. C **31**, 295 (1986).
[7] T. Hambye and K. Riesselmann, Phys. Rev. D **55**, 7255 (1997).
[8] M. Sher, Phys. Rep. **179**, 273 (1989).
[9] M. Lindner, M. Sher, and H. W. Zaglauer, Phys. Lett. B **228**, 139 (1989).
[10] C. Ford, D. R. T. Jones, P. W. Stephenson, and M. B. Einhorn, Nucl. Phys. **B395**, 17 (1993).
[11] M. Sher, Phys. Lett. B **317**, 159 (1993); **331**, 448(A) (1994).
[12] G. Altarelli and G. Isidori, Phys. Lett. B **337**, 141 (1994).
[13] J. A. Casas, J. R. Espinosa, and M. Quiros, Phys. Lett. B **342**, 171 (1995); **382**, 374 (1996).
[14] G. Degrassi, S. Di Vita, J. Elias-Miro, J. R. Espinosa, G. F. Giudice, G. Isidori, and A. Strumia, J. High Energy Phys. 08 (2012) 098.
[15] F. Bezrukov, M. Y. Kalmykov, B. A. Kniehl, and M. Shaposhnikov, J. High Energy Phys. 10 (2012) 140.
[16] D. Buttazzo, G. Degrassi, P. P. Giardino, G. F. Giudice, F. Sala, A. Salvio, and A. Strumia, J. High Energy Phys. 12 (2013) 089.
[17] J. R. Espinosa and M. Quiros, Phys. Lett. B **353**, 257 (1995).
[18] G. F. Giudice, Naturally speaking: The naturalness criterion and physics at the LHC, in *Perspectives on LHC Physics*, edited by G. Kane and A. Pierce (World Scientific, Singapore, 2008), p. 155.
[19] J. D. Wells, Stud. Hist. Phil. Mod. Phys. **49**, 102 (2015).
[20] T. D. Lee, Phys. Rev. D **8**, 1226 (1973).
[21] G. C. Branco, P. M. Ferreira, L. Lavoura, M. N. Rebelo, M. Sher, and J. P. Silva, Phys. Rep. **516**, 1 (2012).

[22] M. Gonderinger, Y. Li, H. Patel, and M. J. Ramsey-Musolf, J. High Energy Phys. 01 (2010) 053.

[23] G. Kreyerhoff and R. Rodenberg, Phys. Lett. B **226**, 323 (1989).

[24] J. Freund, G. Kreyerhoff, and R. Rodenberg, Phys. Lett. B **280**, 267 (1992).

[25] B. M. Kastening, arXiv:hep-ph/9307224.

[26] S. Nie and M. Sher, Phys. Lett. B **449**, 89 (1999).

[27] S. Kanemura, T. Kasai, and Y. Okada, Phys. Lett. B **471**, 182 (1999).

[28] P. M. Ferreira and D. R. T. Jones, J. High Energy Phys. 08 (2009) 069.

[29] J. Elias-Miro, J. R. Espinosa, G. F. Giudice, H. M. Lee, and A. Strumia, J. High Energy Phys. 06 (2012) 031.

[30] O. Lebedev, Eur. Phys. J. C **72**, 2058 (2012).

[31] G. M. Pruna and T. Robens, Phys. Rev. D **88**, 115012 (2013).

[32] R. Costa, A. P. Morais, M. O. P. Sampaio, and R. Santos, Phys. Rev. D **92**, 025024 (2015).

[33] N. Chakrabarty, U. K. Dey, and B. Mukhopadhyaya, J. High Energy Phys. 12 (2014) 166.

[34] D. Das and I. Saha, Phys. Rev. D **91**, 095024 (2015).

[35] D. Chowdhury and O. Eberhardt, arXiv:1503.08216.

[36] J. F. Gunion and H. E. Haber, Phys. Rev. D **67**, 075019 (2003).

[37] H. E. Haber, in *Proceedings of the Toyama International Workshop on Higgs as a Probe of New Physics 2013 (HPNP2013), Toyama, Japan, 2013*, http://www.slac.stanford.edu/econf/C130213.1/.

[38] A. Pich and P. Tuzon, Phys. Rev. D **80**, 091702 (2009); M. Jung, A. Pich, and P. Tuzon, J. High Energy Phys. 11 (2010) 003.

[39] S. Davidson and H. E. Haber, Phys. Rev. D **72**, 035004 (2005); **72**, 099902(E) (2005).

[40] L. J. Hall and M. B. Wise, Nucl. Phys. **B187**, 397 (1981).

[41] V. D. Barger, J. L. Hewett, and R. J. N. Phillips, Phys. Rev. D **41**, 3421 (1990).

[42] M. Aoki, S. Kanemura, K. Tsumura, and K. Yagyu, Phys. Rev. D **80**, 015017 (2009).

[43] P. M. Ferreira, L. Lavoura, and J. P. Silva, Phys. Lett. B **688**, 341 (2010).

[44] G. C. Branco, L. Lavoura, and J. P. Silva, *CP Violation* (Oxford University Press, New York, 1999), Chap. 22.

[45] H. E. Haber and D. O'Neil, Phys. Rev. D **74**, 015018 (2006); **74**, 059905(E) (2006).

[46] H. E. Haber and D. O'Neil, Phys. Rev. D **83**, 055017 (2011).

[47] S. L. Glashow and S. Weinberg, Phys. Rev. D **15**, 1958 (1977).

[48] E. A. Paschos, Phys. Rev. D **15**, 1966 (1977).

[49] H. E. Haber, G. L. Kane, and T. Sterling, Nucl. Phys. **B161**, 493 (1979).

[50] J. F. Donoghue and L. F. Li, Phys. Rev. D **19**, 945 (1979).

[51] F. Mahmoudi and O. Stal, Phys. Rev. D **81**, 035016 (2010).

[52] P. Minkowski, Phys. Lett. B **67**, 421 (1977); M. Gell-Mann, P. Ramond, and R. Slansky, in *Supergravity*, edited by D. Freedman and P. van Nieuwenhuizen (North Holland, Amsterdam, 1979), p. 315; T. Yanagida, Prog. Theor. Phys. **64**, 1103 (1980); R. N. Mohapatra and G. Senjanovic, Phys. Rev. Lett. **44**, 912 (1980); R. N. Mohapatra and G. Senjanovic, Phys. Rev. D **23**, 165 (1981).

[53] N. G. Deshpande and E. Ma, Phys. Rev. D **18**, 2574 (1978).

[54] I. P. Ivanov, Phys. Rev. D **75**, 035001 (2007); **76**, 039902(E) (2007).

[55] K. G. Chetyrkin, J. H. Kuhn, and M. Steinhauser, Comput. Phys. Commun. **133**, 43 (2000); B. Schmidt and M. Steinhauser, Comput. Phys. Commun. **183**, 1845 (2012).

[56] K. A. Olive *et al.* (Particle Data Group Collaboration), Chin. Phys. C **38**, 090001 (2014).

[57] J. Bijnens, J. Lu, and J. Rathsman, J. High Energy Phys. 05 (2012) 118.

[58] H. Arason, D. J. Castano, B. Keszthelyi, S. Mikaelian, E. J. Piard, P. Ramond, and B. D. Wright, Phys. Rev. D **46**, 3945 (1992).

[59] M. K. Parida and B. Purkayastha, Eur. Phys. J. C **14**, 159 (2000).

[60] C. R. Das and M. K. Parida, Eur. Phys. J. C **20**, 121 (2001).

[61] H. E. Haber and R. Hempfling, Phys. Rev. D **48**, 4280 (1993).

[62] I. P. Ivanov, Phys. Rev. D **77**, 015017 (2008).

[63] F. Nagel, Ph.D. thesis, University of Heidelberg, 2004, [http://www.ub.uni-heidelberg.de/archiv/4803]; M. Maniatis, A. von Manteuffel, O. Nachtmann, and F. Nagel, Eur. Phys. J. C **48**, 805 (2006).

[64] C. C. Nishi, Phys. Rev. D **74**, 036003 (2006); **76**, 119901(E) (2007); **76**, 055013 (2007); **77**, 055009 (2008).